

Imbalanced Weak MHD Turbulence

Yoram Lithwick and Peter Goldreich

130-33 Caltech, Pasadena, CA 91125; yoram@tapir.caltech.edu, pmg@gps.caltech.edu

ABSTRACT

MHD turbulence consists of waves that propagate along magnetic fieldlines, in both directions. When two oppositely directed waves collide, they distort each other, without changing their respective energies. In weak MHD turbulence, a given wave suffers many collisions before cascading. “Imbalance” means that more energy is going in one direction than the other. In general, MHD turbulence is imbalanced. A number of complications arise for the imbalanced cascade that are unimportant for the balanced one.

We solve weak MHD turbulence that is imbalanced. Of crucial importance is that the energies going in both directions are forced to equalize at the dissipation scale. We call this the “pinning” of the energy spectra. It affects the entire inertial range.

Weak MHD turbulence is particularly interesting because perturbation theory is applicable. Hence it can be described with a simple kinetic equation. Galtier et al. (2000) derived this kinetic equation. We present a simpler, more physical derivation, based on the picture of colliding wavepackets. In the process, we clarify the role of the zero-frequency mode. We also explain why Goldreich & Sridhar claimed that perturbation theory is inapplicable, and why this claim is wrong. (Our “weak” is equivalent to Goldreich & Sridhar’s “intermediate.”)

We perform numerical simulations of the kinetic equation to verify our claims. We construct simplified model equations that illustrate the main effects. Finally, we show that a large magnetic Prandtl number does not have a significant effect, and that hyperviscosity leads to a pronounced bottleneck effect.

Subject headings: MHD—turbulence

1. Introduction

MHD turbulence is ubiquitous in astrophysics. For example, it is present in the sun, the solar wind, the interstellar medium, molecular clouds, accretion disks, and galaxy clusters. Theoretical understanding of incompressible MHD turbulence has grown explosively in the last decade. Nonetheless, it remains underdeveloped.

Iroshnikov (1963) and Kraichnan (1965) developed a theory for MHD turbulence. They realized that the magnetic field at the largest lengthscale in a cascade directly affects all of the smaller

lengthscales. Small-scale fluctuations can be treated as small-amplitude waves in the presence of a large mean magnetic field. By contrast, the large-scale velocity is unimportant for small-scale dynamics; it can be eliminated by a change of variables, since the equations of MHD are invariant under Galilean transformations.¹

Despite their realization of the importance of the mean magnetic field, Iroshnikov and Kraichnan assumed that small-scale fluctuations are isotropic. Numerical simulations later showed that this assumption is wrong. Even with isotropic excitation at large scales, fluctuations on smaller scales are elongated along the mean magnetic field (e.g., Montgomery & Turner 1981, Shebalin, Matthaeus, & Montgomery 1983).

In retrospect, it is not very surprising to find elongated fluctuations. Arbitrary disturbances in incompressible MHD can be decomposed into shear-Alfvén and pseudo-Alfvén waves. Each wave travels either up or down the mean field at the Alfvén speed, v_A , which is the magnitude of the mean field in velocity units. Consider stirring a magneto-fluid with a spoon that is moving at speed $v \ll v_A$, for a time comparable to the spoon’s width divided by v .² Alfvén waves are radiated away from the spoon, parallel to the mean field with speed $\pm v_A$. After the disturbance is finished, there are two wavepackets travelling away from each other. Each wavepacket is elongated along the mean field, with parallel-to-transverse aspect ratio $\sim v_A/v \gg 1$.

The characteristics of MHD turbulence depend critically on the amount of elongation. When parallel-to-transverse aspect ratios are smaller than v_A/v , waves collide many times before cascading. Hence the turbulence is “weak,” and perturbation theory can be used to derive a kinetic equation and a spectrum (Sridhar & Goldreich 1994; see Zakharov, L’vov, & Falkovich 1992 for a general review of weak turbulence). Goldreich & Sridhar (1997) and Ng & Bhattacharjee (1997) deduced the spectrum of the balanced weak cascade from scaling arguments.³ However, similar

¹One outgrowth of Iroshnikov and Kraichnan’s theory that is particularly relevant to the present paper is Grappin, Pouquet, and Léorat (1983). We discuss it in §4.

²In a turbulent cascade, one would expect $v \ll v_A$ on small scales, since v decreases towards small scales, whereas v_A is unchanged.

³We relegate some of the history to a footnote because it can be confusing. Sridhar & Goldreich (1994) developed the first theory of MHD turbulence that accounted for the anisotropy of fluctuations. They claimed that “three-wave” processes vanish in weak MHD turbulence, and “four-wave” processes must be considered (i.e., perturbation theory is trivial to first order, so second order terms are important). As a result, they used four-wave couplings to derive a kinetic equation and a spectrum for weak MHD turbulence. Montgomery & Matthaeus (1995) claimed, and Ng & Bhattacharjee (1996) showed, that Sridhar & Goldreich (1994) are wrong, and three-wave processes do not vanish. Goldreich & Sridhar (1997) explained the contradiction: Sridhar & Goldreich (1994) had unknowingly assumed that fieldline wander is limited, i.e., that the separation between any two fieldlines is nearly constant along their entire length; in this case, three-wave couplings are negligible and the kinetic equation based on four-wave couplings is correct. In the more realistic case that fieldlines do wander, three-wave processes are important. Goldreich & Sridhar (1997) went on to argue that, in the latter case, perturbation theory is inappropriate, and couplings of all order are of comparable magnitude; so they called this “intermediate” turbulence. Galtier et al. (2000) argued that perturbation theory is appropriate, even when three-wave processes are important. In the Appendix of the present paper, we use

scaling arguments are inadequate for the imbalanced cascade (see §3.2 of the present paper). Galtier et al. (2000) derived the kinetic equation for the weak imbalanced cascade. Their balanced spectrum agrees with that of Goldreich & Sridhar (1997) and Ng & Bhattacharjee (1997). They also presented a partial solution for the general imbalanced case. In §3.2, we explain why their solution is incomplete; in §4 we give the complete solution.

Even if aspect ratios are smaller than v_A/v on large scales, at a small enough scale they become comparable to v_A/v . Below this scale perturbation theory breaks down, and weak turbulence becomes “strong.” Goldreich & Sridhar (1995) worked out the scalings for the balanced strong cascade. They argued that aspect ratios are comparable to v_A/v at all scales in the strong regime. Strong turbulence is difficult, largely because it is non-perturbative. Although strong and weak turbulence differ in a number of ways, they also share many similarities. One of our motivations for studying weak turbulence is to gain insight into strong turbulence. In particular, turbulence in the solar wind is observed to be imbalanced; it cannot be understood without a theory for imbalanced strong MHD turbulence. Yet this theory is unknown. In a future paper, we will work it out by extending the results of the present paper.

2. Basic Equations

Ideal incompressible MHD⁴ is described by the following equations of motion:

$$\partial_t \mathbf{v} + \mathbf{v} \cdot \nabla \mathbf{v} = -\nabla P + \mathbf{B} \cdot \nabla \mathbf{B} , \quad (1)$$

$$\partial_t \mathbf{B} + \mathbf{v} \cdot \nabla \mathbf{B} = \mathbf{B} \cdot \nabla \mathbf{v} , \quad (2)$$

$$\nabla \cdot \mathbf{v} = \nabla \cdot \mathbf{B} = 0 . \quad (3)$$

The density is set to unity; the fluid velocity is \mathbf{v} ; the magnetic field in velocity units is $\mathbf{B} \equiv (\text{magnetic field})/(4\pi)^{1/2}$; the total pressure is $P \equiv p + B^2/2$, which is the sum of the thermal and magnetic pressures. Viscous and resistive terms are neglected in the above equations; they are important on small scales, and will be included where required.

We decompose the magnetic field into its mean, $v_A \hat{\mathbf{z}}$, where v_A is the Alfvén speed and $\hat{\mathbf{z}}$ is a unit vector, and into its fluctuating part $\mathbf{b} \equiv \mathbf{B} - v_A \hat{\mathbf{z}}$. With this decomposition, the equations of motion may be written in terms of the Elsasser variables, $\mathbf{w}^\uparrow \equiv \mathbf{v} - \mathbf{b}$ and $\mathbf{w}^\downarrow \equiv \mathbf{v} + \mathbf{b}$, as follows:

$$\partial_t \mathbf{w}^\uparrow + v_A \partial_z \mathbf{w}^\uparrow = -\mathbf{w}^\downarrow \cdot \nabla \mathbf{w}^\uparrow - \nabla P , \quad (4)$$

$$\partial_t \mathbf{w}^\downarrow - v_A \partial_z \mathbf{w}^\downarrow = -\mathbf{w}^\uparrow \cdot \nabla \mathbf{w}^\downarrow - \nabla P , \quad (5)$$

$$\nabla \cdot \mathbf{w}^\uparrow = \nabla \cdot \mathbf{w}^\downarrow = 0 . \quad (6)$$

Goldreich & Sridhar’s picture of wavepackets following wandering fieldlines to clarify the controversy, and to explain why perturbation theory works. Because it does work, we call the cascade “weak” instead of “intermediate.”

⁴In this paper, we consider only incompressible MHD turbulence; compressibility does not alter the dynamics very much (Lithwick & Goldreich 2001).

Note that P is not an independent degree of freedom. Taking the divergence of either equation (4) or (5) yields

$$P = -\nabla^{-2}(\nabla \mathbf{w}^\uparrow : \nabla \mathbf{w}^\downarrow), \quad (7)$$

where ∇^{-2} is the inverse Laplacian. When $\mathbf{w}^\downarrow = 0$, \mathbf{w}^\uparrow propagates undistorted upwards along the mean magnetic field with speed v_A . Similarly, when $\mathbf{w}^\uparrow = 0$, \mathbf{w}^\downarrow propagates downwards at v_A . Nonlinear interactions occur only between oppositely directed wavepackets. It is these interactions that are responsible for turbulence.

There are three conserved quantities in incompressible MHD. Two of these are immediately apparent from equations (4)-(6): the energies of the upgoing and of the downgoing waves, i.e., $(w^\uparrow)^2$ and $(w^\downarrow)^2$. Technically, these are twice the energy per unit mass. We refer to them as simply energies throughout the paper. These energies are directly related to the total (kinetic plus magnetic) energy $\propto (w^\uparrow)^2 + (w^\downarrow)^2$ and to the cross-helicity $\propto (w^\uparrow)^2 - (w^\downarrow)^2$. The focus of this paper is turbulence where the energies in the up and down waves differ, or, equivalently, where the cross-helicity is non-zero. The third conserved quantity is magnetic helicity; however, we consider only non-helical turbulence in this paper, so helicity does not play a role.

In MHD turbulence, on lengthscales much smaller than the outer scale, there is effectively a strong mean magnetic field that is due to fluctuations on the largest lengthscales. Gradients transverse to this mean field are much larger than gradients along it (e.g., Shebalin, Matthaeus, & Montgomery 1983, Goldreich & Sridhar 1995, 1997, Ng & Bhattacharjee 1996). This allows the MHD equations to be slightly simplified. Denoting transverse components with the symbol $\perp \equiv (x, y)$, the transverse components of equation (4) are

$$\partial_t \mathbf{w}_\perp^\uparrow + v_A \partial_z \mathbf{w}_\perp^\uparrow \approx -\mathbf{w}_\perp^\downarrow \cdot \nabla_\perp \mathbf{w}_\perp^\uparrow - \nabla_\perp P, \quad (8)$$

assuming that $w_z^\downarrow \partial_z \mathbf{w}^\uparrow$ is much smaller than $\mathbf{w}_\perp^\downarrow \cdot \nabla_\perp \mathbf{w}^\uparrow$, and equation (6) is

$$\nabla_\perp \cdot \mathbf{w}_\perp^\uparrow \approx 0. \quad (9)$$

We assume that the parallel components of \mathbf{w}^\uparrow and \mathbf{w}^\downarrow are either comparable to, or less than, their respective perpendicular components. We will see below that this is typically the case in the inertial range of a turbulent cascade. Similarly,

$$\partial_t \mathbf{w}_\perp^\downarrow - v_A \partial_z \mathbf{w}_\perp^\downarrow \approx -\mathbf{w}_\perp^\uparrow \cdot \nabla_\perp \mathbf{w}_\perp^\downarrow - \nabla_\perp P, \quad (10)$$

$$\nabla_\perp \cdot \mathbf{w}_\perp^\downarrow \approx 0. \quad (11)$$

If we change \approx to $=$, equations (8)-(11) form a closed set. They are called the equations of reduced MHD. They apply also in compressible MHD whenever transverse gradients are larger than parallel ones (e.g., Biskamp 1993). The main goal of this paper is to solve these equations. Although the complete equations are not much more complicated, it simplifies our discussions to neglect parallel

gradients relative to perpendicular ones at the outset. There are two conserved energies in reduced MHD: $(w_{\perp}^{\uparrow})^2$ and $(w_{\perp}^{\downarrow})^2$.

The parallel components of equations (4) and (5) are

$$\partial_t w_z^{\uparrow} + v_A \partial_z w_z^{\uparrow} \approx -\mathbf{w}_{\perp}^{\downarrow} \cdot \nabla_{\perp} w_z^{\uparrow}, \quad (12)$$

$$\partial_t w_z^{\downarrow} - v_A \partial_z w_z^{\downarrow} \approx -\mathbf{w}_{\perp}^{\uparrow} \cdot \nabla_{\perp} w_z^{\downarrow}, \quad (13)$$

after neglecting parallel gradients relative to transverse ones, and after assuming that $|w_z^{\uparrow}|$ and $|w_z^{\downarrow}|$ are not much smaller than $|\mathbf{w}_{\perp}^{\uparrow}|$ and $|\mathbf{w}_{\perp}^{\downarrow}|$. Clearly, $(w_z^{\uparrow})^2$ and $(w_z^{\downarrow})^2$ are conserved quantities. The transverse equations describing reduced MHD are unaffected by these parallel equations because the former are independent of w_z^{\uparrow} and w_z^{\downarrow} . Nonetheless, the parallel equations have observable consequences.

It is conventional to decompose the normal modes of linearized incompressible MHD, \mathbf{w}^{\uparrow} and \mathbf{w}^{\downarrow} , into shear-Alfvén and pseudo-Alfvén waves. These correspond to the Alfvén and slow waves of compressible MHD. When perpendicular gradients are much larger than parallel ones, $\mathbf{w}_{\perp}^{\uparrow}$ and $\mathbf{w}_{\perp}^{\downarrow}$ are nearly equivalent to shear-Alfvén waves; w_z^{\uparrow} and w_z^{\downarrow} are nearly equivalent to pseudo-Alfvén waves.

Also observationally relevant is the evolution of a passive scalar s , which satisfies $\partial_t s + \mathbf{v} \cdot \nabla s = 0$. In terms of Elsasser variables, and after neglecting parallel gradients, the passive scalar satisfies

$$\partial_t s \approx -(1/2)(\mathbf{w}_{\perp}^{\uparrow} + \mathbf{w}_{\perp}^{\downarrow}) \cdot \nabla_{\perp} s. \quad (14)$$

To avoid a proliferation of subscripts, in the remainder of this paper we drop the \perp from $\mathbf{w}_{\perp}^{\uparrow}$ and $\mathbf{w}_{\perp}^{\downarrow}$. To denote the parallel components, we use w_z^{\uparrow} and w_z^{\downarrow} .

3. Weak MHD Turbulence: Heuristic Discussion

One of the virtues of weak MHD turbulence is that it can be analyzed in a mathematically rigorous way with perturbation theory; this yields a kinetic equation. Nevertheless, we begin with a qualitative description, which captures most of the features of the turbulent cascade.

3.1. Scaling Relation

MHD turbulence can be understood from the dynamics of \mathbf{w}^{\uparrow} and \mathbf{w}^{\downarrow} (eqs. [8-11] for reduced MHD, dropping \perp subscripts). To linear order, \mathbf{w}^{\uparrow} is a wave that propagates up the mean magnetic fieldlines at the Alfvén speed, v_A ; \mathbf{w}^{\downarrow} propagates down at v_A . Each wave perturbs the mean magnetic fieldlines. Nonlinear terms describe the interaction between oppositely directed waves:

each wave nearly follows the fieldlines perturbed by its collision partner.⁵

Consider an upgoing wavepacket that encounters a train of downgoing wavepackets. As the upgoing wave travels up the length of the downgoing train, it is gradually distorted. It tries to follow the perturbed fieldlines in the downgoing train, but these fieldlines “wander,” i.e., the transverse separation between any two fieldlines changes. When the up-wave has travelled through a sufficiently large number of downgoing wavepackets that the amount of fieldline wander is comparable to the up-wave’s transverse size, then the up-wave cascades.

To be quantitative, let each downgoing wave in the train have a typical amplitude w_λ^\downarrow , a transverse size λ , and a parallel size Λ , where “transverse” and “parallel” refer to the orientation relative to the mean magnetic field. The most important collisions are between wavepackets of comparable transverse size (see §4.3.1). So let the upgoing wave have transverse size λ as well.

Since each downgoing wavepacket has a typical perturbed magnetic field of magnitude $\sim w_\lambda^\downarrow$ (neglecting the factor of 1/2), it bends the fieldlines by the angle w_λ^\downarrow/v_A ; the transverse displacement of a fieldline through this wavepacket is $(w_\lambda^\downarrow/v_A)\Lambda$; and the wander of two typical fieldlines through the wavepacket, if they are initially separated by λ , is also $(w_\lambda^\downarrow/v_A)\Lambda$.

In weak turbulence, the wander through a single wavepacket is smaller than the wavepacket’s transverse size,

$$\frac{w_\lambda^\downarrow}{v_A}\Lambda \ll \lambda \quad \text{and} \quad \frac{w_\lambda^\uparrow}{v_A}\Lambda \ll \lambda. \quad (15)$$

When these inequalities are not satisfied, strong turbulence is applicable; see §4.3.2. Thus in weak turbulence an upgoing wavepacket must travel through many downgoing ones before cascading. After N downgoing wavepackets, fieldlines have wandered a distance $\sim N^{1/2}(w_\lambda^\downarrow/v_A)\Lambda$, assuming that wavepackets are statistically independent. The upgoing wavepacket is fully distorted—and hence cascaded—when the fieldlines it is following wander a distance λ , i.e., when $N \sim (\lambda v_A/\Lambda w_\lambda^\downarrow)^2$. Since each downgoing wavepacket is crossed in the time Λ/v_A , the cascade time of the upgoing wavepacket is

$$t_{\text{cas}}^\uparrow \sim \left(\frac{\lambda v_A}{\Lambda w_\lambda^\downarrow}\right)^2 \frac{\Lambda}{v_A} \sim \left(\frac{\lambda}{w_\lambda^\downarrow}\right)^2 \frac{v_A}{\Lambda}. \quad (16)$$

In this time, the upgoing wavepacket travels a distance $v_A t_{\text{cas}}^\uparrow$, which is much larger than its own length, Λ .⁶ The head and the tail of the upgoing wavepacket are both distorted by the same

⁵The equation for a scalar quantity f that travels upwards at speed v_A , while following the magnetic fieldlines of the down-going \mathbf{w}^\downarrow is $(\partial_t + v_A \partial_z + \mathbf{w}^\downarrow \cdot \nabla_\perp) f = 0$. Equation (8) for the vector \mathbf{w}^\uparrow differs from this because of the pressure term, which is required to keep \mathbf{w}^\uparrow incompressible, while conserving the energy $(w^\uparrow)^2$. Thus \mathbf{w}^\uparrow does not exactly follow the fieldlines of \mathbf{w}^\downarrow . Nonetheless, this deviation does not greatly affect the behaviour of the turbulence. Dissipation is a second effect that prevents the following of fieldlines. In the present discussion, we consider lengthscales that are sufficiently large that dissipation can be neglected.

⁶We assume throughout this paper that the upgoing waves’ parallel lengthscale is the same as that of the downgoing waves, Λ ; the extension to the case when they differ is trivial, as long as the inequalities (15) are both satisfied, with

downgoing wavepackets; so both head and tail undergo nearly the same distortion as they cascade.⁷ Consequently, as the upgoing wavepacket cascades to smaller transverse lengthscales, it does not cascade to smaller parallel ones:

$$\Lambda = \text{scale independent} . \quad (17)$$

A proof of this follows from the 3-wave resonance relations (Shebalin, Matthaeus, & Montgomery 1983; see also §A.5 of the present paper).

We calculate the steady state energy spectra by using Kolmogorov’s picture of energy flowing from large to small lengthscales. The energy in up-waves flows from lengthscales larger than λ to those smaller than λ at the rate

$$\epsilon^\uparrow \sim \frac{(w_\lambda^\uparrow)^2}{t_{\text{cas}}^\uparrow} \sim \left[\frac{w_\lambda^\uparrow w_\lambda^\downarrow}{\lambda} \right]^2 \frac{\Lambda}{v_A} . \quad (18)$$

We call this simply the “flux.” We define ϵ^\uparrow more precisely below (eq. [51]). In steady state, the flux must be independent of λ , so

$$w_\lambda^\uparrow w_\lambda^\downarrow \propto \lambda . \quad (19)$$

3.2. Insufficiency of Scaling Arguments for the Imbalanced Cascade

A balanced cascade has $w_\lambda^\uparrow = w_\lambda^\downarrow \equiv w_\lambda$. Its solution in steady state is simple: $w_\lambda \propto \lambda^{1/2}$ and $\epsilon^\uparrow = \epsilon^\downarrow \sim w_\lambda^4 \Lambda / \lambda^2 v_A$ (Goldreich & Sridhar 1997, Ng & Bhattacharjee 1997). However, if the cascade is imbalanced, a number of complications arise.

By the symmetry between up- and down-going waves, the down-going flux is given by the analogue of equation (18):

$$\epsilon^\downarrow \sim \left[\frac{w_\lambda^\uparrow w_\lambda^\downarrow}{\lambda} \right]^2 \frac{\Lambda}{v_A} . \quad (20)$$

Because ϵ^\uparrow and ϵ^\downarrow both depend on the same combination of w_λ^\uparrow and w_λ^\downarrow —namely their product—the steady state solution is non-trivial. Had this degeneracy not occurred, e.g., had we found

$$\epsilon^\uparrow \sim \frac{(w_\lambda^\uparrow)^{2+\gamma} (w_\lambda^\downarrow)^{2-\gamma}}{\lambda^2} \frac{\Lambda}{v_A} \quad \text{and} \quad \epsilon^\downarrow \sim \frac{(w_\lambda^\uparrow)^{2-\gamma} (w_\lambda^\downarrow)^{2+\gamma}}{\lambda^2} \frac{\Lambda}{v_A} , \quad (21)$$

where $\gamma \neq 0$, then the solution would have been simple: $w_\lambda^\uparrow \propto w_\lambda^\downarrow \propto \lambda^{1/2}$ and $(\epsilon^\uparrow / \epsilon^\downarrow) \sim (w_\lambda^\uparrow / w_\lambda^\downarrow)^{2\gamma}$, which follow from the constancy of ϵ^\uparrow and ϵ^\downarrow with λ .

the appropriate Λ ’s.

⁷The head of the upgoing wavepacket slightly distorts each downgoing wavepacket; so the downgoing wavepacket seen by the tail is slightly distorted relative to that seen by the head. Nonetheless, this backreaction is a higher-order correction that can be ignored in weak turbulence; see §A.1.

But in weak MHD turbulence $\gamma = 0$ (eqs. [18] and [20]); constancy of ϵ^\downarrow with λ is forced by the constancy of ϵ^\uparrow , and does not yield new information. One implication is that scaling arguments are insufficient to determine the flux ratio $\epsilon^\uparrow/\epsilon^\downarrow$. Physically, any flux ratio should be possible. But without the dimensionless coefficients of equations (18) and (20), $\epsilon^\uparrow/\epsilon^\downarrow$ cannot be determined. The coefficients cannot be obtained from scaling arguments; they depend on the spectral slopes of w_λ^\uparrow and w_λ^\downarrow (which are related through $w_\lambda^\uparrow w_\lambda^\downarrow \propto \lambda$, eq. [19]). Galtier et al. (2000) calculated the coefficients using kinetic equations. We explain how in §A.4. Therefore these authors were able to relate the flux ratio to the spectral slopes.

The arguments presented thus far are still insufficiently constraining. Equations (18) and (20) constrain only the product $w_\lambda^\uparrow w_\lambda^\downarrow$. There are seemingly an infinite number of solutions with given values of ϵ^\uparrow and ϵ^\downarrow , since w_λ^\uparrow can be multiplied by any constant as long as w_λ^\downarrow is divided by this same constant. Furthermore, we expect on physical grounds that if the values of w_λ^\uparrow and w_λ^\downarrow at a given lengthscale are fixed (instead of the values of ϵ^\uparrow and ϵ^\downarrow), the cascade should be completely constrained; however, in this case the constancy of equations (18) and (20) leaves the λ -dependence of $w_\lambda^\uparrow/w_\lambda^\downarrow$ completely undetermined—even given the coefficients derived by Galtier et al. (2000). Do w_λ^\uparrow and w_λ^\downarrow cross? Are they cut off by dissipation at the same scale? All of these problems for the imbalanced cascade can be resolved once the dynamics at the dissipation scale is understood.

3.3. Dynamics at the Dissipation Scale: Pinned Spectra

The main result of the present paper is that the energies of the up- and down-going waves are forced to equalize—they are “pinned”—at the dissipation scale. This completely constrains the cascade. It is unusual that the dynamics at the dissipation scale has such an important influence. In this subsection we explain why pinning occurs. In §4, we give the resulting solution of the steady state cascade.

From equation (16), the cascade time of the up-going waves is inversely proportional to the energy of the down-going ones: $t_{\text{cas}}^\uparrow = (\lambda/w_\lambda^\downarrow)^2(v_A/\Lambda)$, and similarly for the downgoing waves. We consider how the spectra evolve if initially, on lengthscales comparable to the dissipation scale, waves going in one direction are more energetic than the oppositely directed ones. To facilitate the discussion, we refer to Figure 1 on page 19, which presents the results from a numerical simulation that we discuss in detail in §6.1. In the middle panels of Figures 1a-d, we plot $e^\uparrow(k) \sim (\lambda w_\lambda^\uparrow)^2$ and $e^\downarrow(k) \sim (\lambda w_\lambda^\downarrow)^2$ as functions of wavenumber $k = 1/\lambda$. The initial condition is shown in Figure 1a. Initially, $w_\lambda^\uparrow > w_\lambda^\downarrow$, so $t_{\text{cas}}^\uparrow > t_{\text{cas}}^\downarrow$. We consider a lengthscale-dependent dissipation time, t_{diss} , that is the same for both up- and down-going waves.⁸ On large lengthscales, the dissipation timescale is much longer than the cascade times; t_{diss} decreases faster with increasing k than both t_{cas}^\uparrow and $t_{\text{cas}}^\downarrow$. The effects of dissipation are felt on lengthscales where t_{diss} is comparable to—or smaller than—

⁸For example, in the simulation presented in Figure 1, $t_{\text{diss}} \simeq \lambda^2/\nu$, where ν is both the viscosity and the resistivity.

either t_{cas}^\uparrow or $t_{\text{cas}}^\downarrow$. Since $t_{\text{cas}}^\uparrow > t_{\text{cas}}^\downarrow$ in the vicinity of the dissipation scale, the largest lengthscale at which dissipation effects are felt is where $t_{\text{cas}}^\uparrow \sim t_{\text{diss}}$. In Figure 1a, this is at $k \sim 4,000$. We now let the spectra evolve; see Figs. 1b-c. We hold the energies at $k \simeq 1$ fixed; this does not affect the short-time behaviour shown in Figs. 1b-c. Since w_λ^\uparrow feels the dissipative effects at $k \sim 4,000$, its spectrum is exponentially cut off at smaller scales. This implies that the cascade time of the down waves, $t_{\text{cas}}^\downarrow$, increases exponentially towards smaller scales. As a result, down-wave energy that is being cascaded from large to small scales cannot be cascaded fast enough at $k \gtrsim 4,000$. Therefore the down-waves' energy flux is backed up, and the w_λ^\downarrow spectrum rises. Furthermore, as w_λ^\downarrow rises, t_{cas}^\uparrow falls, so the cascade time of the up-waves on small scales decreases, and the up-wave spectrum falls. The final result is that the two spectra are pinned at the dissipation scale. This pinning occurs very quickly: on the dissipation timescale.

4. Steady State Energy Spectra

In steady state, the energy spectra w_λ^\uparrow and w_λ^\downarrow are power laws that (i) are pinned at the dissipation scale, and (ii) satisfy $w_\lambda^\uparrow w_\lambda^\downarrow \propto \lambda$ (eq. [19]). These two conditions completely characterize the steady state spectra, as long as w_λ^\uparrow and w_λ^\downarrow are specified at the outer scale. It is a remarkable feature of weak MHD turbulence that the dynamics at the dissipation scale dramatically affects the entire cascade. Normally, the energy in turbulent cascades is viewed as flowing unimpeded from larger scales to smaller scales. Energy is injected at the outer scale and swallowed up at the dissipation scale. But in weak MHD turbulence, if initially the spectra are not pinned, then the spectrum with lower energy becomes backed up, and its energy increases until pinning occurs.

A similar effect was found by Grappin, Pouquet, and Léorat (1983).⁹ These authors modelled imbalanced MHD turbulence with an EDQNM closure approximation. However, they assumed that the turbulence is isotropic, which is incorrect. Nonetheless, they found in their model that scaling arguments constrained only the sum of the slopes of the up- and down-going waves' spectra, and that the two spectra are constrained to be equal at the dissipation scale. Thus they discovered pinning, even though they analyzed an invalid model of MHD turbulence.

In the remainder of this section, we derive the scalings in steady state. We denote the dissipation scale by λ_{diss} , and the value of w_λ^\uparrow and w_λ^\downarrow at λ_{diss} by w_{diss} . We can then express the energy spectra as follows

$$w_\lambda^\uparrow = w_{\text{diss}} \left(\frac{\lambda}{\lambda_{\text{diss}}} \right)^{(1+\alpha)/2} \quad (22)$$

$$w_\lambda^\downarrow = w_{\text{diss}} \left(\frac{\lambda}{\lambda_{\text{diss}}} \right)^{(1-\alpha)/2} . \quad (23)$$

These spectra are valid in the ‘‘inertial range,’’ i.e., on lengthscales larger than the dissipation scale,

⁹We thank Bill Matthaeus for pointing out this reference to us.

and smaller than the outer scale. There are three parameters that must be calculated to constrain the spectra: w_{diss} , λ_{diss} , and α .

For definiteness, we assume that dissipation is caused by a diffusive process, described by a viscous term of the form $\nu \nabla^2 \mathbf{v}$ in equation (1) and a resistive term of the form $\nu \nabla^2 \mathbf{B}$ in equation (2). This implies that the magnetic Prandtl number is equal to one.¹⁰ The dissipative timescale is

$$t_{\text{diss}}(\lambda) \simeq \frac{\lambda^2}{\nu}. \quad (24)$$

At the dissipation scale, the cascade time is equal to t_{diss} , i.e., $t_{\text{cas}}(\lambda_{\text{diss}}) = t_{\text{diss}}(\lambda_{\text{diss}})$, which implies that

$$\frac{\lambda_{\text{diss}}^2}{\nu} \simeq \left(\frac{\lambda_{\text{diss}}}{w_{\text{diss}}} \right)^2 \frac{v_A}{\Lambda}, \quad (25)$$

after using equations (16) and (24); so

$$w_{\text{diss}} \simeq \left(\frac{\nu v_A}{\Lambda} \right)^{1/2}. \quad (26)$$

Thus when the dissipation is caused by a diffusive process, w_{diss} is independent of the outer-scale energies and the inertial-range fluxes. This is not true for λ_{diss} or α .

To calculate λ_{diss} and α , we consider two alternative scenarios: specified energies at the outer scale, and specified fluxes.

4.1. Fixed Energies at the Outer Scale

Suppose that the energies are specified at the outer scale, λ_{out} , where w_{λ}^{\uparrow} and w_{λ}^{\downarrow} are denoted by $w_{\lambda_{\text{out}}}^{\uparrow}$ and $w_{\lambda_{\text{out}}}^{\downarrow}$. Since $w_{\lambda}^{\uparrow} w_{\lambda}^{\downarrow} / \lambda = w_{\text{diss}}^2 / \lambda_{\text{diss}}$,

$$\lambda_{\text{diss}} \simeq \frac{\lambda_{\text{out}}}{w_{\lambda_{\text{out}}}^{\uparrow} w_{\lambda_{\text{out}}}^{\downarrow}} \frac{\nu v_A}{\Lambda}, \quad (27)$$

after using equation (26).

Dividing equation (22) by equation (23) yields $w_{\lambda_{\text{out}}}^{\uparrow} / w_{\lambda_{\text{out}}}^{\downarrow} = (\lambda_{\text{out}} / \lambda_{\text{diss}})^{\alpha}$, so

$$\alpha = \frac{\ln [w_{\lambda_{\text{out}}}^{\uparrow} / w_{\lambda_{\text{out}}}^{\downarrow}]}{\ln [\lambda_{\text{out}} / \lambda_{\text{diss}}]} \simeq \frac{\ln [w_{\lambda_{\text{out}}}^{\uparrow} / w_{\lambda_{\text{out}}}^{\downarrow}]}{\ln [w_{\lambda_{\text{out}}}^{\uparrow} w_{\lambda_{\text{out}}}^{\downarrow} \Lambda / (\nu v_A)]}. \quad (28)$$

With $w_{\lambda_{\text{out}}}^{\uparrow} / w_{\lambda_{\text{out}}}^{\downarrow}$ fixed, the cascade is balanced ($\alpha \rightarrow 0$) in the limit that the inertial range is infinitely large ($\lambda_{\text{out}} / \lambda_{\text{diss}} \rightarrow \infty$).

¹⁰It is straightforward to consider other forms for the dissipation. We consider magnetic Prandtl numbers greater than unity in §8, and hyperviscosity in §9.

Inserting equations (26), (27), and (28) into the spectra (eqs. [22] and [23]) gives the solution to the steady state imbalanced weak cascade, assuming that $w_{\lambda_{\text{out}}}^{\uparrow}$ and $w_{\lambda_{\text{out}}}^{\downarrow}$ are specified.

Although we have solved for the spectra, recall from §3.2 that heuristic arguments are insufficient for calculating the ratio of the fluxes that are carried by these spectra, $\epsilon^{\uparrow}/\epsilon^{\downarrow}$. In the following subsection, we show how $\epsilon^{\uparrow}/\epsilon^{\downarrow}$ is related to the spectra. This relation is particularly important for solving the inverse problem: given the fluxes ϵ^{\uparrow} and ϵ^{\downarrow} , what are the spectra of w_{λ}^{\uparrow} and w_{λ}^{\downarrow} ?

4.2. Fixed Fluxes

Physically, we expect that when the fluxes are fixed, the cascade should be completely constrained. In this subsection, we solve for the spectra given ϵ^{\uparrow} and ϵ^{\downarrow} . To accomplish this, the dimensionless coefficients of equations (18) and (20) are required. For a given power-law solution, $w_{\lambda}^{\uparrow} \propto \lambda^{(1+\alpha)/2}$ and $w_{\lambda}^{\downarrow} \propto \lambda^{(1-\alpha)/2}$, these coefficients depend on α :

$$\epsilon^{\uparrow} = f(\alpha) \left[\frac{w_{\lambda}^{\uparrow} w_{\lambda}^{\downarrow}}{\lambda} \right]^2 \frac{\Lambda}{v_A}, \quad (29)$$

$$\epsilon^{\downarrow} = f(-\alpha) \left[\frac{w_{\lambda}^{\uparrow} w_{\lambda}^{\downarrow}}{\lambda} \right]^2 \frac{\Lambda}{v_A}, \quad (30)$$

where $f(\alpha)$ is a dimensionless function of α that must be calculated. By the symmetry between up and down waves, ϵ^{\uparrow} and ϵ^{\downarrow} are both proportional to the same function f , evaluated at $\pm\alpha$. Since heuristic arguments are insufficient to calculate the function f , it is fortunate that weak turbulence can be analyzed with perturbation theory. Galtier et al. (2000) computed f . We compute it in equation (A29) in the Appendix.

The ratio of the fluxes is related to α by

$$\frac{\epsilon^{\uparrow}}{\epsilon^{\downarrow}} = \frac{f(\alpha)}{f(-\alpha)}. \quad (31)$$

The limit $|\alpha| \ll 1$ is particularly interesting. For given outer-scale energies, if the inertial range is very large then the steady state cascade is nearly balanced (see the discussion below eq. [28]), and $|\alpha| \ll 1$. In this limit, we show in the Appendix that $f(\alpha) \simeq f(0) \cdot (1 + 0.5\alpha)$ (see eq. [A30]). Thus

$$\frac{\epsilon^{\uparrow}}{\epsilon^{\downarrow}} - 1 \simeq \alpha, \quad |\alpha| \ll 1. \quad (32)$$

To linear order in α , the product of the fluxes is independent of α :

$$\epsilon^{\uparrow} \epsilon^{\downarrow} \simeq [f(0)]^2 \left[\frac{w_{\lambda}^{\uparrow} w_{\lambda}^{\downarrow}}{\lambda} \right]^4 \left(\frac{\Lambda}{v_A} \right)^2 = [f(0)]^2 \left[\frac{w_{\text{diss}}^2}{\lambda_{\text{diss}}} \right]^4 \left(\frac{\Lambda}{v_A} \right)^2, \quad |\alpha| \ll 1. \quad (33)$$

In the Appendix, we show that $f(0) = 1.87$ (eq. A31). Although for most purposes the precise value of $f(0)$ is unimportant, we shall need it when discussing our numerical simulations.

To summarize, in the limit of small $|\alpha|$, if ϵ^\uparrow and ϵ^\downarrow are specified, then the spectra of w_λ^\uparrow and w_λ^\downarrow are given by equations (22) and (23), with w_{diss} , α , and λ_{diss} given by equations (26), (32), and (33). Note that, to first order in α , the only relation that depends on the kinetic equation is equation (32).¹¹

If, instead of specifying ϵ^\uparrow and ϵ^\downarrow , we specify the outer scale energies—in which case the spectra are given in §4.1—then equations (32) and (33) give the resulting fluxes.

4.3. Three Peripheral Issues

This subsection may be skipped on a first reading, as it does not impact our main line of argument.

4.3.1. Locality

In §3.1, it is assumed that the dominant interactions are those between wavepackets that have comparable transverse lengthscales, i.e., interactions are “local” in lengthscale. In this section, we justify this assumption.

We focus on the cascading of an upgoing wavepacket by downgoing ones. Let the upgoing wavepacket have transverse size λ , and let the downgoing wavepackets each have transverse size l , parallel size Λ , and amplitude w_l^\downarrow . The upgoing wavepacket cascades when the fieldlines it is following wander a distance comparable to its transverse size, λ .

We consider first the case that $l < \lambda$. Two fieldlines that are separated by λ at the head of the downgoing wavepackets wander independently of each other. Their transverse separation after N downgoing wavepackets increases by

$$N^{1/2}(w_l^\downarrow/v_A)\Lambda \quad , \quad l < \lambda \quad . \quad (34)$$

Conversely, if $l > \lambda$, then the magnetic field can be expanded to linear order in λ , so the magnetic field at two points separated by λ differs by $\sim w_l^\downarrow\lambda/l$. Consequently, the fieldlines separate by

$$N^{1/2}(w_l^\downarrow/v_A)(\lambda/l)\Lambda \quad , \quad l > \lambda \quad , \quad (35)$$

so long as this separation is smaller than λ .

For interactions to be local, i.e., for the amount of fieldline wander seen by an up-wave of transverse size λ to be maximized by those down-waves that have $l \sim \lambda$, the following two conditions

¹¹Aside from the uninteresting dependence of equation (33) on $f(0)$.

must hold: (i) w_l^\downarrow is an increasing function of l (eq. [34]); and (ii) w_l^\downarrow/l is a decreasing function of l (eq. [35]). So the cascade is local if

$$0 < \frac{d \ln w_\lambda^\downarrow}{d \ln \lambda} < 1 . \quad (36)$$

The same condition clearly holds for w_λ^\uparrow . In terms of the steady-state scalings, $w_\lambda^\uparrow \propto \lambda^{(1+\alpha)/2}$ and $w_\lambda^\downarrow \propto \lambda^{(1-\alpha)/2}$, the condition

$$-1 < \alpha < 1 \quad (37)$$

is required for the cascade to be local; otherwise, nonlocal effects are important. Galtier et al. (2000) derived the inequalities in (37) from their kinetic equation.

There is a second reason why the condition $d \ln w_\lambda^\uparrow / d \ln \lambda < 1$ is necessary for our heuristic arguments to be valid. Consider a single Fourier mode with wavelength l and amplitude w_l^\uparrow ; then the typical difference in w^\uparrow between two points separated by $\lambda < l$ is $\sim w_l^\uparrow \lambda / l$, expanding to linear order in λ . So, if the condition $d \ln w_\lambda^\uparrow / d \ln \lambda < 1$ is violated, then the contribution to w_λ^\uparrow (i.e., to the typical difference in w^\uparrow between two points separated by λ) is dominated by those Fourier modes that have wavelengths $l \gg \lambda$. This is a different kind of non-locality than considered previously: the upgoing energy that crosses lengthscale λ comes directly from much larger scales (with $l \gg \lambda$).

4.3.2. Transition to Strong Turbulence

Weak turbulence is applicable when $w_\lambda^\downarrow \Lambda / v_A \ll \lambda$ and $w_\lambda^\uparrow \Lambda / v_A \ll \lambda$ (eq. [15]). Since λ decreases faster than both w_λ^\downarrow and w_λ^\uparrow (eq. [36]), even if these inequalities are satisfied at large lengthscales, they are violated at small ones. Thus weak turbulence has a limited inertial range.

Strong turbulence, which is applicable when the above inequalities are violated, is of greater relevance than weak turbulence for describing astrophysical sites such as the solar wind. In strong turbulence the change in fieldline separation within a single wavepacket is not smaller than the transverse size of the wavepacket. This has two implications. First, equation (16) for the cascade time is no longer valid; and second, the parallel size of wavepackets Λ decreases towards smaller scales because the head and tail of a wavepacket are independently cascaded. The balanced strong cascade is worked out by Goldreich & Sridhar (1995); we discuss the imbalanced strong cascade in a future paper. Strong turbulence is more difficult to analyze than weak turbulence because it does not submit to perturbation theory. Nonetheless, a number of the features of weak turbulence that we develop in the present paper are applicable to strong turbulence. This is one of our motivations for studying the weak cascade.

Since this paper is concerned with weak turbulence, we choose the dissipation scale to be sufficiently large that the entire cascade is weak, i.e., we require that

$$\frac{w_{\lambda_{\text{diss}}}^\uparrow \Lambda}{v_A \lambda_{\text{diss}}} \ll 1 , \quad (38)$$

and similarly for $w_{\lambda_{\text{diss}}}^{\downarrow}$. Using equations (26) and (27), we can re-write this condition as follows:

$$\frac{w_{\lambda_{\text{out}}}^{\uparrow} w_{\lambda_{\text{out}}}^{\downarrow}}{v_A^2} \ll \frac{\lambda_{\text{out}}}{\Lambda} \left(\frac{\nu}{\Lambda v_A} \right)^{1/2}. \quad (39)$$

There is also a lower limit on the product of the outer scale energies, set by the requirement that the dissipation scale be smaller than the outer scale, which implies that

$$\frac{w_{\lambda_{\text{out}}}^{\uparrow} w_{\lambda_{\text{out}}}^{\downarrow}}{v_A^2} \gg \frac{\nu}{\Lambda v_A}, \quad (40)$$

(see eq. [27]). Typically, one expects that $\Lambda \sim \lambda_{\text{out}}$, so as long as $\nu \ll \Lambda v_A$, the above two inequalities can be satisfied with appropriately chosen $w_{\lambda_{\text{out}}}^{\uparrow} w_{\lambda_{\text{out}}}^{\downarrow}$.

4.3.3. The Steady State Spectra of w_z^{\uparrow} and w_z^{\downarrow} and of a Passive Scalar

In §2 we showed that the parallel components w_z^{\uparrow} and w_z^{\downarrow} do not affect the evolution of the perpendicular components, \mathbf{w}^{\uparrow} and \mathbf{w}^{\downarrow} .¹² By contrast, the perpendicular components control the evolution of the parallel ones.

The steady state spectra of the parallel components can be derived as follows. By analogy between the equation for w_z^{\uparrow} (eq. [13]) and that for \mathbf{w}^{\uparrow} (eq. [8]), the cascade time of w_z^{\uparrow} is similar to that of \mathbf{w}^{\uparrow} , i.e., it is given by $t_{\text{cas}}^{\uparrow}$ (see eq. [16]). We denote the typical amplitude of the parallel component of the up-wave on lengthscale λ by $w_{z,\lambda}^{\uparrow}$. The cascade rate of the energy of the parallel component is $(w_{z,\lambda}^{\uparrow})^2/t_{\text{cas}}^{\uparrow}$; in steady state it must be independent of λ . Comparing this to the cascade rate of the perpendicular component, $(w_{\lambda}^{\uparrow})^2/t_{\text{cas}}^{\uparrow}$, which must also be independent of λ , we deduce

$$w_{z,\lambda}^{\uparrow} \propto w_{\lambda}^{\uparrow}. \quad (41)$$

Note that the evolution equation for w_z^{\uparrow} (eq. [13]) is linear. So the overall amplitude of the $w_{z,\lambda}^{\uparrow}$ spectrum is arbitrary; more accurately, it is set by the value of $w_{z,\lambda}^{\uparrow}$ at the outer scale. Of course, a similar relation holds for the down-waves:

$$w_{z,\lambda}^{\downarrow} \propto w_{\lambda}^{\downarrow}. \quad (42)$$

Finally, we consider the spectrum of a passive scalar, s , whose evolution is described by equation (14). From this equation, it is apparent that the cascade time of the passive scalar is given by either $t_{\text{cas}}^{\uparrow}$ or $t_{\text{cas}}^{\downarrow}$, whichever is shorter. So, by the same reasoning that we used in deriving equation (41), we deduce

$$s_{\lambda} \propto \min(w_{\lambda}^{\uparrow}, w_{\lambda}^{\downarrow}), \quad (43)$$

¹²Recall that we drop the \perp label.

where s_λ is the typical value of s on lengthscale λ . Because of the pinning of the spectra, the lesser of the two spectra w_λ^\uparrow and w_λ^\downarrow is also the flatter. So s_λ is proportional to the flatter of w_λ^\uparrow and w_λ^\downarrow .

5. Kinetic Equations in Weak Turbulence

Weak turbulence can be analyzed with perturbation theory. As a consequence, the evolution of the energy spectra of the up- and down-waves is described by a closed set of two equations; in other words, the two-point correlation functions evolve independently of all higher-order correlation functions. This is a great simplification.

Evolution equations for the energy spectra—the “kinetic equations”—were obtained in Galtier et al. (2000, 2001). We present an alternate, more physical, derivation in the Appendix. Such a derivation is useful because it clears up a number of erroneous claims that have been made in the literature—in particular, the claim of Goldreich & Sridhar (1997) that perturbation theory is inapplicable.

In the following, we summarize the result derived in the Appendix. The kinetic equations are given in Fourier-space. We Fourier transform $\mathbf{w}^\uparrow(x, y, z, t)$ and $\mathbf{w}^\downarrow(x, y, z, t)$ in x and y (but not z), and denote the transforms by $\mathbf{w}_\mathbf{k}^\uparrow(z, t)$ and $\mathbf{w}_\mathbf{k}^\downarrow(z, t)$, where \mathbf{k} is purely transverse ($k_z \equiv 0$). We define the energy spectra e^\uparrow and e^\downarrow such that

$$\langle \mathbf{w}_\mathbf{k}^\uparrow(z, t) \cdot \mathbf{w}_{\mathbf{k}'}^\uparrow(z, t) \rangle = e^\uparrow(k, t) \delta(\mathbf{k} + \mathbf{k}') \quad (44)$$

$$\langle \mathbf{w}_\mathbf{k}^\downarrow(z, t) \cdot \mathbf{w}_{\mathbf{k}'}^\downarrow(z, t) \rangle = e^\downarrow(k, t) \delta(\mathbf{k} + \mathbf{k}') , \quad (45)$$

where $\delta(\mathbf{k})$ is a two-dimensional Dirac delta-function, and angled brackets denote both an ensemble average and an average over z . (We assume that the turbulence is homogeneous in z .) Both e^\uparrow and e^\downarrow are real. The turbulence is isotropic in the transverse plane, so e^\uparrow and e^\downarrow are functions of the magnitude of \mathbf{k} .

From equation (A24) in the Appendix, the kinetic equation for the up-waves is

$$\frac{\partial}{\partial t} \Big|_k e^\uparrow(k, t) = \frac{\Lambda}{v_A} k^2 \int_0^\infty dk_2 k_2^3 \left[e^\uparrow(k_2, t) - e^\uparrow(k, t) \right] \int_0^{2\pi} d\theta \sin^2 \theta \cos^2 \theta \frac{e^\downarrow(k_1, t)}{k_1^2} - \nu k^2 e^\uparrow(k, t) \quad (46)$$

where

$$k_1 \equiv (k^2 + k_2^2 - 2kk_2 \cos \theta)^{1/2} . \quad (47)$$

We have included a term describing diffusive dissipation on small lengthscales, $-\nu k^2 e^\uparrow$, where ν is the viscosity, which is assumed to be equal to the resistivity.

Because of the symmetry between up- and down-waves, the equation for e^\downarrow is the same as that for e^\uparrow , but with \uparrow and \downarrow everywhere switched. The steady-state relation between the energy and the flux that we use above (eq. [29]) is obtained in the Appendix by setting the right-hand side of equation (46) zero.

Within an order-unity factor, $k^2 e^\uparrow \sim (w_\lambda^\uparrow)^2$ when $\lambda = 1/k$. Recall from §3 that w_λ^\uparrow is the “typical” value of \mathbf{w}^\uparrow on lengthscale λ ; more precisely, it can be defined as the square root of the second-order structure function of \mathbf{w}^\uparrow . Therefore the steady-state scaling $w_\lambda^\uparrow \propto \lambda^{(1+\alpha)/2}$ (eq. [22]) corresponds to $e^\uparrow \propto k^{-(3+\alpha)}$; similarly, $w_\lambda^\downarrow \propto \lambda^{(1-\alpha)/2}$ corresponds to $e^\downarrow \propto k^{-(3-\alpha)}$.

5.1. Energy and Flux in the Kinetic Equation

The energy per unit mass in up-waves is $\langle |\mathbf{w}^\uparrow|^2 \rangle / 2 = (1/2)(2\pi)^{-4} \int e^\uparrow d^2\mathbf{k}$. So e^\uparrow is proportional to the energy per unit $d^2\mathbf{k}$. Conservation of up-wave energy implies that $(d/dt) \int (ke^\uparrow) dk = 0$, assuming isotropy and neglecting dissipation. This can be seen immediately from equation (46) if we re-write it as follows (without the diffusive term),

$$(\partial/\partial t)(ke_k^\uparrow) = (\Lambda/v_A) \int_0^\infty (e_{k_2}^\uparrow - e_k^\uparrow) S^\downarrow(k, k_2) dk_2, \quad (48)$$

since S^\downarrow is symmetric,

$$S^\downarrow(k, k_2) \equiv (kk_2)^3 \int_0^{2\pi} \sin^2 \theta \cos^2 \theta e_{k_1}^\downarrow k_1^{-2} = S^\downarrow(k_2, k), \quad (49)$$

and $e_2^\uparrow - e_k^\uparrow$ is antisymmetric. In comparing our results with those of Galtier et al. (2000), note that these authors use the energy per unit k , which they denote E^+ , i.e., $E^+ \sim ke^\uparrow$, within a multiplicative constant.

The energy flux ϵ^\uparrow is the net rate at which energy flows across a given wavenumber k . We define it as the integral of the right-hand side of equation (46) over $d^2\mathbf{k}/(2\pi)$, from some particular k to infinity, so that the kinetic equation can be written as

$$(\partial/\partial t)(ke_k^\uparrow) = -(\partial/\partial k)\epsilon^\uparrow. \quad (50)$$

Explicitly, we can write the flux in the form

$$\epsilon^\uparrow = \int_0^k dp \int_k^\infty dq (e_p^\uparrow - e_q^\uparrow) S^\downarrow(p, q). \quad (51)$$

It is trivial to verify that $\partial/\partial k$ of this expression is equal to minus the right-hand side of equation (46). The positive term in equation (51) is the rate at which energy flows from wavenumbers smaller than k to those greater than k ; the negative term is similar, but with the origin and destination of the energy switched.

6. Numerical Simulations of Kinetic Equations

In this section we present the results of numerical simulations which verify our previous heuristic discussions: in particular, the pinning of spectra and the scaling of the spectra in steady state.

It is much faster to simulate kinetic equations than the full equations of motion for w^\uparrow and w^\downarrow . There are a number of reasons for this. First, the kinetic equations are only one dimensional, since homogeneity has been assumed parallel to the mean magnetic field, and isotropy has been assumed in the plane transverse to the mean magnetic field. Second, and more importantly, the averaged energies e^\uparrow and e^\downarrow are much smoother functions of k than w^\uparrow and w^\downarrow . Thus, a logarithmically-spaced grid can be used, which greatly reduces the number of variables that need to be evolved. The result is an enormous reduction in computational time. A typical kinetic simulation takes a few hours on a PC to reach steady state. A comparable fully three-dimensional MHD simulation, would require many months, if not years, on the fastest supercomputers.

Galtier et al. (2000) perform numerical simulations of the kinetic equation. However, their investigation of the imbalanced cascade is incomplete. In particular, they only plot spectra of the product $e^\uparrow e^\downarrow$. They do not discuss the pinning of the spectra at the dissipation scale, which is crucial to the evolution of the cascade.

For our numerical simulations of the kinetic equations (eq. [46] and the analogous e^\downarrow equation), we set

$$\frac{\Lambda}{v_A} = \frac{1}{2} . \quad (52)$$

This corresponds to absorbing $2\Lambda/v_A$ into e^\uparrow and e^\downarrow . Our method of integration is very similar to that of Galtier et al. (2000). We change variables in equation (46) to give

$$\frac{\partial}{\partial t} \Big|_k e^\uparrow(k, t) = k \int_0^\infty dk_2 k_2^2 \left[e^\uparrow(k_2, t) - e^\uparrow(k, t) \right] \int_{|k-k_2|}^{|k+k_2|} dk_1 \sin \theta \cos^2 \theta \frac{e^\downarrow(k_1, t)}{k_1} - \nu k^2 e^\uparrow(k, t) , \quad (53)$$

where θ is a function of k_1 and k_2 (given in eq. [47]). We evaluate all functions of k on a fixed, logarithmically-spaced grid with $k = 2^{i/8}$, $i = 1, \dots, 100$. At the outer scale,

$$k_{\text{out}} = 2^{1/8} = 1.09 , \quad (54)$$

and the maximum k is

$$k_{\text{max}} = 2^{100/8} = 5793 . \quad (55)$$

The double integral over k_1 and k_2 is performed by summing the values of the integrand evaluated on the k -space grid. The factor $\sin \theta \cos^2 \theta$ is averaged in the vicinity of each grid point, i.e., at each (k_1, k_2) . Since θ is a function of k_1/k and k_2/k , and since the grid is logarithmic, the averaged angular factor can be precomputed and stored in a two-dimensional matrix, each element of which is the average in the vicinity of $(k_1/k, k_2/k)$.¹³ We integrate in time with second-order Runge-Kutta.

¹³In evaluating the integral near k_{out} , the values of $e^\uparrow(k_2 < k_{\text{out}})$ and $e^\downarrow(k_1 < k_{\text{out}})$ are required. Since these values are off of the grid, some method of extrapolation is needed. In the runs that we present in this paper, we extrapolate with $e^\uparrow, e^\downarrow \propto k^{-2}$. With this extrapolation, there is no energy transfer from modes with $k < k_{\text{out}}$ to those with $k > k_{\text{out}}$; steeper extrapolations would transfer energy. We have also experimented with a flatter spectrum for $k < k_{\text{out}}$: $e^\uparrow = e^\uparrow(k_{\text{out}})$, $e^\downarrow = e^\downarrow(k_{\text{out}})$. While this changes the behaviour near $k \sim k_{\text{out}}$ —in particular, it leads to a

For the discussions of the simulations that follow, recall that the energies of the waves at a given lengthscale $\lambda = 1/k$ are, within unimportant multiplicative constants,

$$(w_\lambda^\uparrow)^2 \sim k^2 e^\uparrow(k) , \quad (w_\lambda^\downarrow)^2 \sim k^2 e^\downarrow(k) . \quad (56)$$

The cascade times of the up- and down-going waves are, respectively,

$$t_{\text{cas}}^\uparrow(k) \sim (k^4 e^\downarrow(k))^{-1} , \quad t_{\text{cas}}^\downarrow(k) \sim (k^4 e^\uparrow(k))^{-1} , \quad (57)$$

(see eq. [16]). The dissipation time is

$$t_{\text{diss}}(k) = (\nu k^2)^{-1} , \quad (58)$$

(see eq. [24]). In the simulations in this section, the viscosity is

$$\nu = 3 \cdot 10^{-5} ; \quad (59)$$

this implies that $t_{\text{diss}}(k_{\text{max}}) = 0.001$.

6.1. Fixed Energies at the Outer Scale

For our first simulation, we fix $e^\uparrow(k_{\text{out}}) = 1$ and $e^\downarrow(k_{\text{out}}) = 0.1$ throughout the simulation. We do this by adding an injection term at $k = k_{\text{out}}$ to the right-hand side of the kinetic equation (eq. [53]). The two injection terms, $\dot{e}_{\text{inj}}^\uparrow$ and $\dot{e}_{\text{inj}}^\downarrow$, are adjusted to keep $e^\uparrow(k_{\text{out}})$ and $e^\downarrow(k_{\text{out}})$ fixed. At the initial time, we set $e^\uparrow \propto k^{-3}$ and $e^\downarrow \propto k^{-3}$ (Fig. 1a). These initial spectra are seemingly valid solutions of the steady-state flux relations (eqs. [29] and [30]), with $\alpha = 0$ and $\epsilon^\uparrow = \epsilon^\downarrow$. But the spectra are not pinned. When they are evolved in time, it seen that they become pinned to each other at the dissipation scale. This pinning happens very quickly—at the dissipation timescale (Fig 1b). The reason for this pinning was discussed in §3.3, and can be traced in Figures 1a-c.

The entire e^\downarrow spectrum adjusts to e^\uparrow on the timescale $t_{\text{cas}}^\downarrow(k_{\text{out}}) \sim 1$. The e^\uparrow spectrum takes longer to adjust, since $t_{\text{cas}}^\uparrow(k_{\text{out}}) \sim 10$. By $t = 50$, steady state is reached (Fig 1d). We discuss the resulting steady state spectra in §6.3. We find that, in steady state, the energy injection rates required to keep the outer scale energies fixed are

$$\dot{e}_{\text{inj}}^\uparrow = 0.136 \quad , \quad \dot{e}_{\text{inj}}^\downarrow = 0.114 \quad ; \quad (60)$$

these values are used in our second simulation.

sharp drop in e^\uparrow and e^\downarrow between $k = k_{\text{out}}$ and $k = 2^{1/8} k_{\text{out}}$ by a factor of around 3—the remainder of the spectrum for $k > 2^{1/8} k_{\text{out}}$ is nearly unaffected. With the k^{-2} extrapolation there is also a drop at $k = k_{\text{out}}$, as can be seen in the top panel of Figure 1d, for example; but this drop is much less drastic than with the flat spectrum extrapolation.

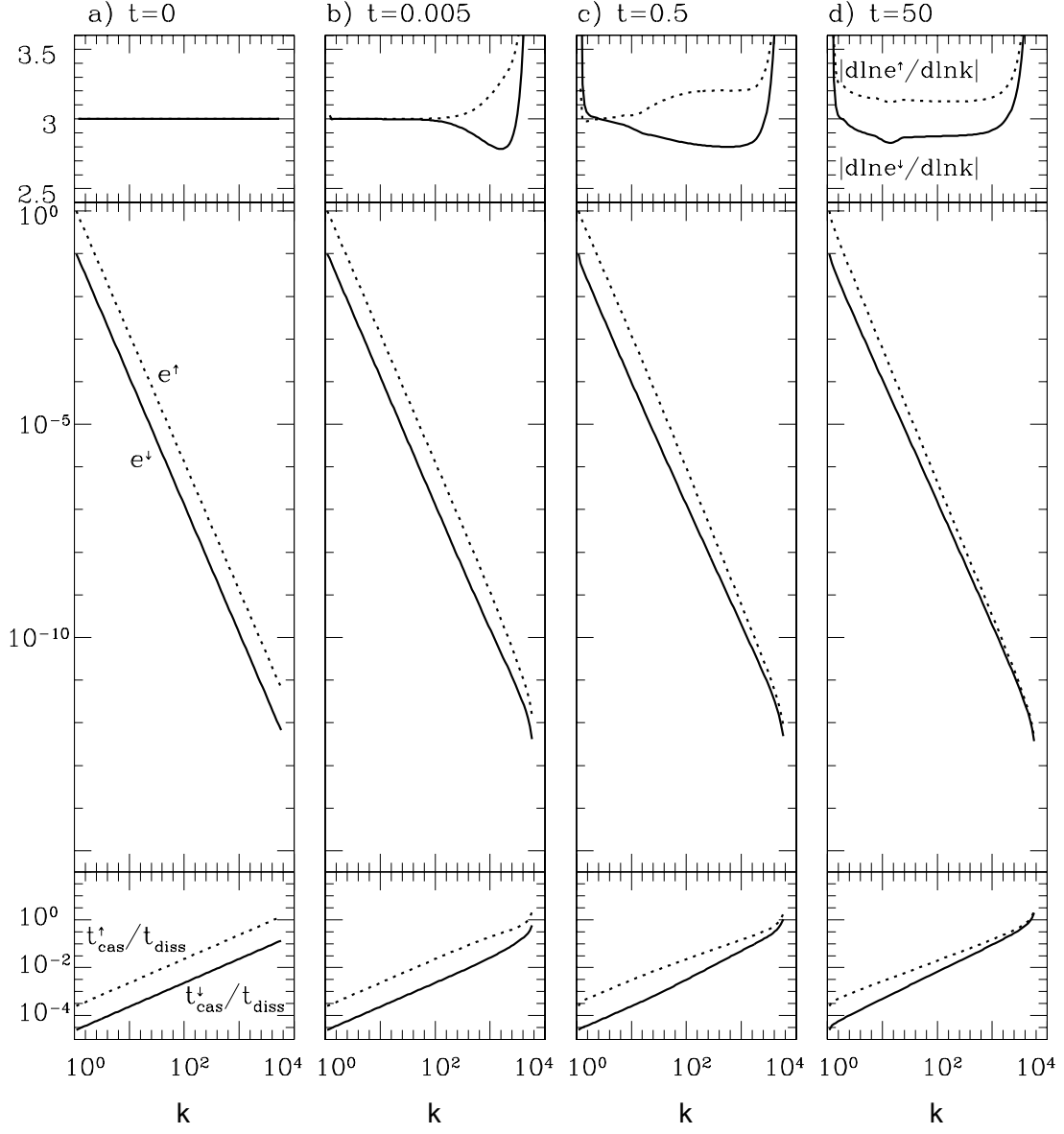


Fig. 1.— Simulation of Kinetic Equations with Fixed Energies at the Outer Scale

6.2. Fixed Fluxes

In our second simulation, we inject energy at fixed rates at $k = k_{\text{out}}$, allowing $e^\uparrow(k_{\text{out}})$ and $e^\downarrow(k_{\text{out}})$ free to evolve. We use the same injection rates as we found in steady state in the previous simulation (eq. [60]). We add to $e^\uparrow(k_{\text{out}})$ and $e^\downarrow(k_{\text{out}})$ at these fixed rates throughout the present simulation. Since we add to $e^\uparrow(k_{\text{out}})$ and $e^\downarrow(k_{\text{out}})$ at the same rate as we did in steady state in the previous simulation, we expect that our second simulation will reach the same steady state as did the first one. We shall show that it does. Note that, strictly speaking, $\dot{e}_{\text{inj}}^\uparrow$ and $\dot{e}_{\text{inj}}^\downarrow$ are not precisely equal to the fluxes. Nonetheless, we ignore this subtlety and refer to the present simulation as one of constant fluxes. We shall evaluate the fluxes more precisely below.

For our initial condition, we use the spectra obtained in steady state in the first simulation, but multiplied by a constant; specifically, $e^\uparrow(k) \rightarrow e^\uparrow(k)/10$ and $e^\downarrow(k) \rightarrow e^\downarrow(k) \cdot 10$ (see Fig. 2a). With these initial spectra, and with the aforementioned fluxes, the flux relations (eqs. [29] and [30]) are satisfied—since they were satisfied before the multiplication and division by 10. But, once again, this is not a valid steady state solution because the spectra are not pinned at the dissipation scale. When the spectra are evolved in time, the spectra are first pinned (Figs. 2a-c). In this simulation, the spectra are initially pinned where $t_{\text{cas}}^\downarrow \sim t_{\text{diss}}$, which is at $k \sim 1,000$. Therefore the pinning timescale is $\sim t_{\text{diss}}(k = 1,000) \sim 0.03$.

As expected, the same steady state is reached as in the first simulation (Fig. 2d). In reaching steady state, the two spectra must cross. This happens at $t \sim 40$, when the two spectra are nearly identical, with slopes equal to -3 , and with outer scale energy equal to ~ 0.3 . The time to reach steady state is considerably longer in the constant flux simulation than in the constant energy one. Steady state is reached at $t \sim 250$, as opposed to $t \sim 50$ in the previous simulation.

6.3. Energies and Fluxes in Steady State

We can quantitatively compare the behaviour in steady state with our calculations in §4. We consider the steady state reached in the two simulations discussed above. Recall that both simulations reach the same steady state, at which point the spectra are as shown in Figures 1d and 2d. For our comparisons, we need the following quantities: $\nu = 3 \cdot 10^{-5}$ (eq. [59]), $k_{\text{out}} = 1.09$ (eq. [54]), $\Lambda/v_A = 1/2$ (eq. [52]), $e^\uparrow(k_{\text{out}}) = 0.63$, and $e^\downarrow(k_{\text{out}}) = 0.066$.¹⁴

From equation (27), the dissipation wavenumber is

$$k_{\text{diss}} = \frac{\Lambda}{\nu v_A} (k_{\text{out}}^6 e^\uparrow(k_{\text{out}}) e^\downarrow(k_{\text{out}}))^{1/2} = 4,400 \quad , \quad (61)$$

¹⁴For our first simulation, we actually fixed $e^\uparrow(k_{\text{out}}) = 1$ and $e^\downarrow(k_{\text{out}}) = 0.1$. However, as we discuss in footnote 13, there is a drop in energy between the first and second grid point. The values $e^\uparrow(k_{\text{out}}) = 0.63$, and $e^\downarrow(k_{\text{out}}) = 0.066$ are found by taking the power laws seen in steady state for $e^\uparrow(k > k_{\text{out}})$ and $e^\downarrow(k > k_{\text{out}})$, and extrapolating them to $k = k_{\text{out}}$.

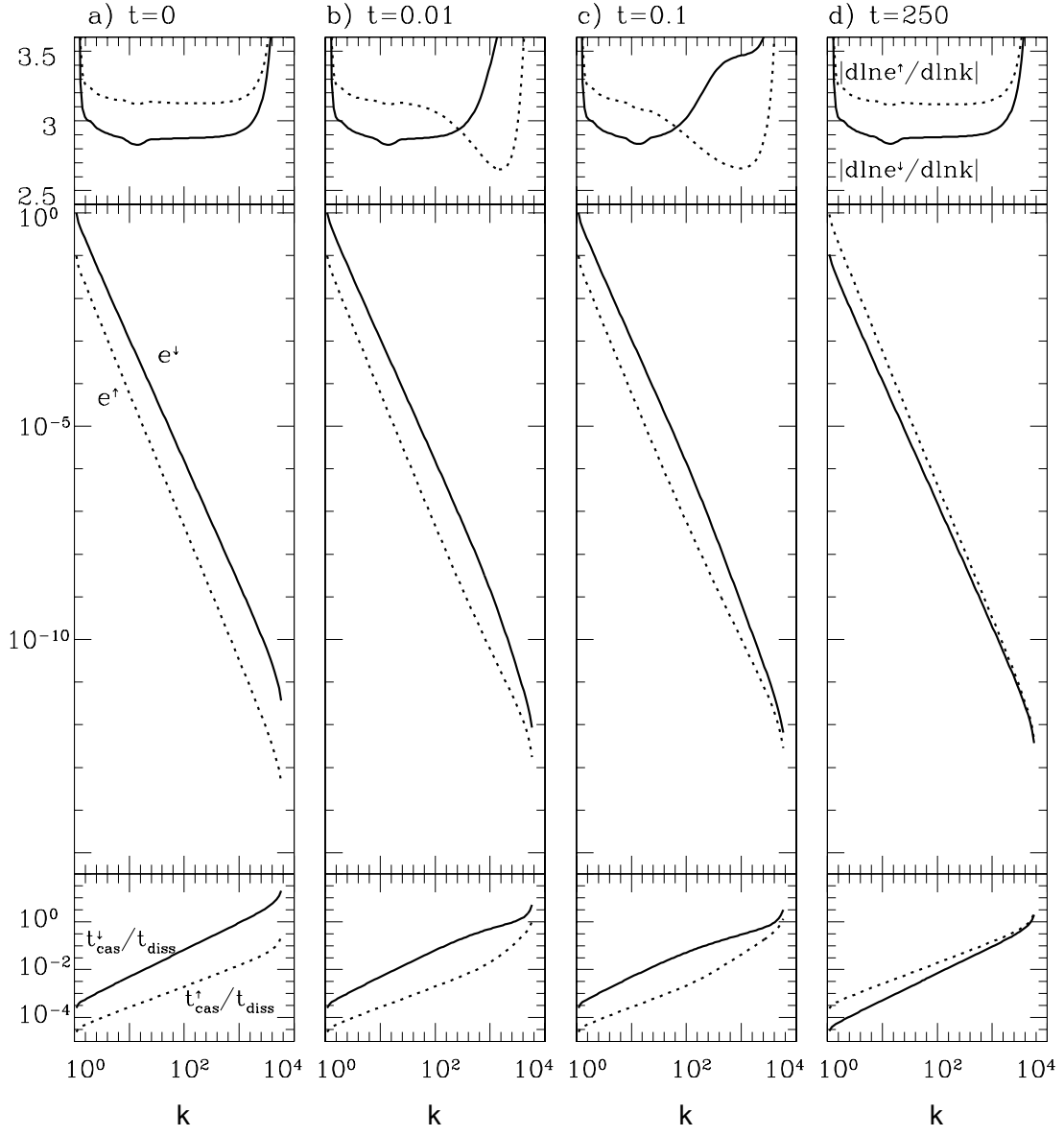


Fig. 2.— Simulation of Kinetic Equations with Fixed Fluxes

in agreement with the value seen in Figure 1d.

Equation (28) gives

$$\alpha = \frac{\ln[e^\uparrow(k_{\text{out}})/e^\downarrow(k_{\text{out}})]}{\ln[k_{\text{out}}^4 e^\uparrow(k_{\text{out}}) e^\downarrow(k_{\text{out}}) (\Lambda/\nu v_A)^2]} = 0.14 , \quad (62)$$

which implies that the steady state slopes should be

$$-\frac{d \ln e^\uparrow}{d \ln k} = 3 + \alpha = 3.14 \quad (63)$$

$$-\frac{d \ln e^\downarrow}{d \ln k} = 3 - \alpha = 2.86 . \quad (64)$$

This is in agreement with the top panel of Figure 1d, which shows that the slope of e^\uparrow in the inertial range, while varying slightly with k , mostly remains between 3.1 and 3.15; the slope of e^\downarrow is between 2.85 and 2.9.

To derive the steady-state formulae that we have used thus far in this section, heuristic arguments suffice. However, to relate energy spectra to fluxes, the kinetic equation is required. From equation (33), we should have

$$\epsilon^\uparrow \epsilon^\downarrow = [1.87 \cdot k_{\text{out}}^6 e^\uparrow(k_{\text{out}}) e^\downarrow(k_{\text{out}}) (\Lambda/v_A)]^2 = 0.0043 , \quad (65)$$

where the numerical factor 1.87 is obtained from the kinetic equation. A more important application of the kinetic equation is to derive the ratio of the fluxes, for which heuristic arguments are useless. From equation (32), we should have

$$\epsilon^\uparrow/\epsilon^\downarrow - 1 = \alpha = 0.14 , \quad (66)$$

when we use the value of α predicted in equation (62). To compare the above predictions for the fluxes (eqs. [65] and [66]) with the fluxes seen in the numerical simulation, we plot the latter in Figure 3. We calculated ϵ^\uparrow with equation (51), using the steady state spectra shown in Figure 1d. The quantity $S^\downarrow(p, q)$ that appears in equation (51) is given in equation (49). Since the kinetic code calculates $S^\downarrow(p, q)$ in order to evolve the kinetic equations (see eq. [53]), it is trivial to modify the code so that it can be used to evaluate the flux. To calculate ϵ^\downarrow , we used the analogue of equation (51), with \uparrow and \downarrow switched. We see in Figure 3 that the fluxes are nearly independent of k in the inertial range, with $\epsilon^\uparrow \simeq 0.070$ and $\epsilon^\downarrow \simeq 0.061$. These values give $\epsilon^\uparrow/\epsilon^\downarrow - 1 \simeq 0.15$, in agreement with equation (66). They also give $\epsilon^\uparrow \epsilon^\downarrow \simeq 0.0043$, in agreement with equation (65).

From Figure 3, dissipation affects ϵ^\uparrow and ϵ^\downarrow for $k \gtrsim 100$. Thus dissipation has a big reach. If we add the dissipation term to the flux-conservation form of the kinetic equation (eq. [50]), then we see that in steady state the kinetic equation must satisfy

$$-\frac{d\epsilon^\uparrow}{d \ln k} = \nu k^4 e^\uparrow . \quad (67)$$

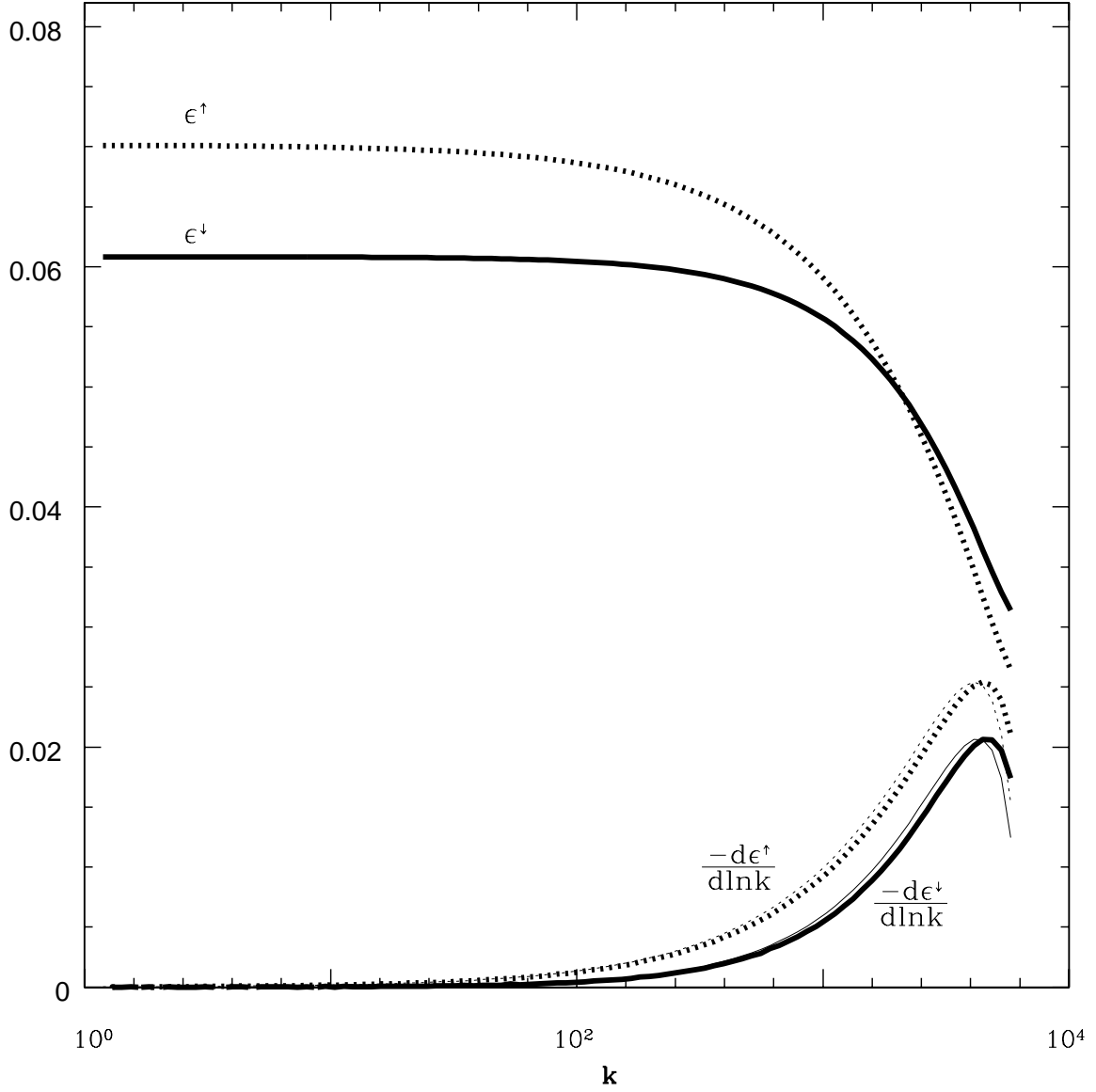


Fig. 3.— Steady State Fluxes and Flux Gradients

Fluxes and flux gradients are shown as bold solid and dotted lines. Also shown as unlabelled thin lines that nearly overlap the flux gradients are $\nu k^4 e^\uparrow$ (thin dotted line) and $\nu k^4 e^\downarrow$ (thin solid line).

The spectra from which the fluxes were extracted are shown in Figure 1d.

The left-hand side of this equation gives the rate of energy increase (per logarithmic band in k) due to the k -space divergence of the flux; in steady state, it must be balanced by the energy loss rate due to dissipation. In Figure 3, we plot $-(d/d \ln k)\epsilon^\uparrow$ as a bold dotted line; we evaluated it by taking the numerical derivative of the displayed ϵ^\uparrow . The quantity $\nu k^4 e^\uparrow$ is the unlabelled thin dotted line that nearly overlaps $-(d/d \ln k)\epsilon^\uparrow$. Thus equation (67) is satisfied in the simulation. The same is true for the down waves, which are shown as solid lines in Figure 3.

6.4. Decaying Turbulence

For our third simulation, we allow the spectra to decay without injecting any energy. The initial condition is the steady state spectra from the previous simulation, see Figure 4. At the outer scale, the cascade time of the down-waves is $\sim 1/e^\uparrow(k_{\text{out}}) \sim 1$, so $e^\downarrow(k_{\text{out}})$ decays on this timescale. More precisely, from the values plotted in Figure 4, $e^\downarrow \propto \exp(-0.5t)$ at fixed k .

The cascade time of the up-waves is much longer. Initially, $t_{\text{cas}}^\uparrow \sim 10$ at the outer scale; as e^\downarrow decays, t_{cas}^\uparrow increases exponentially. So $e^\uparrow(k_{\text{out}})$ does not evolve. At larger k 's, e^\uparrow is cut off by dissipation; the dissipation wavenumber is $\sim (\nu t)^{-1/2} \sim 200t^{-1/2}$.

The spectra appear to evolve in a self-similar manner, with the spectra remaining pinned at their dissipation scale. The end result is that the energy in the down-waves disappears, while the energy in the up-waves is nearly unchanged. Decaying weak turbulence is unstable: an initial imbalance between up and down waves is magnified exponentially. A similar instability occurs in strong turbulence, as suggested by Dobrowolny et al. (1980) in the context of the solar wind, and as seen in numerical simulations of strong turbulence (Maron & Goldreich 2001, and Cho et al. 2002).

7. A Model of the Kinetic Equations: Coupled Diffusion Equations

It is instructive to model the kinetic equations with two coupled diffusion equations. Investigation of these model equations illustrates that the pinning of spectra is quite general; the only requirement is that the cascade time of one type of wave be inversely related to the energy of the other type. A second reason for considering model equations is that they can be simulated much faster and more easily than the kinetic equations. Finally, by contrasting the kinetic equations with the model equations, we can gain insight into the behaviour of the kinetic equations.

7.1. Derivation of Coupled Diffusion Equations

Our model equation is

$$\frac{\partial}{\partial t} k e^\uparrow = -\frac{\partial}{\partial k} \tilde{\epsilon}^\uparrow, \quad (68)$$

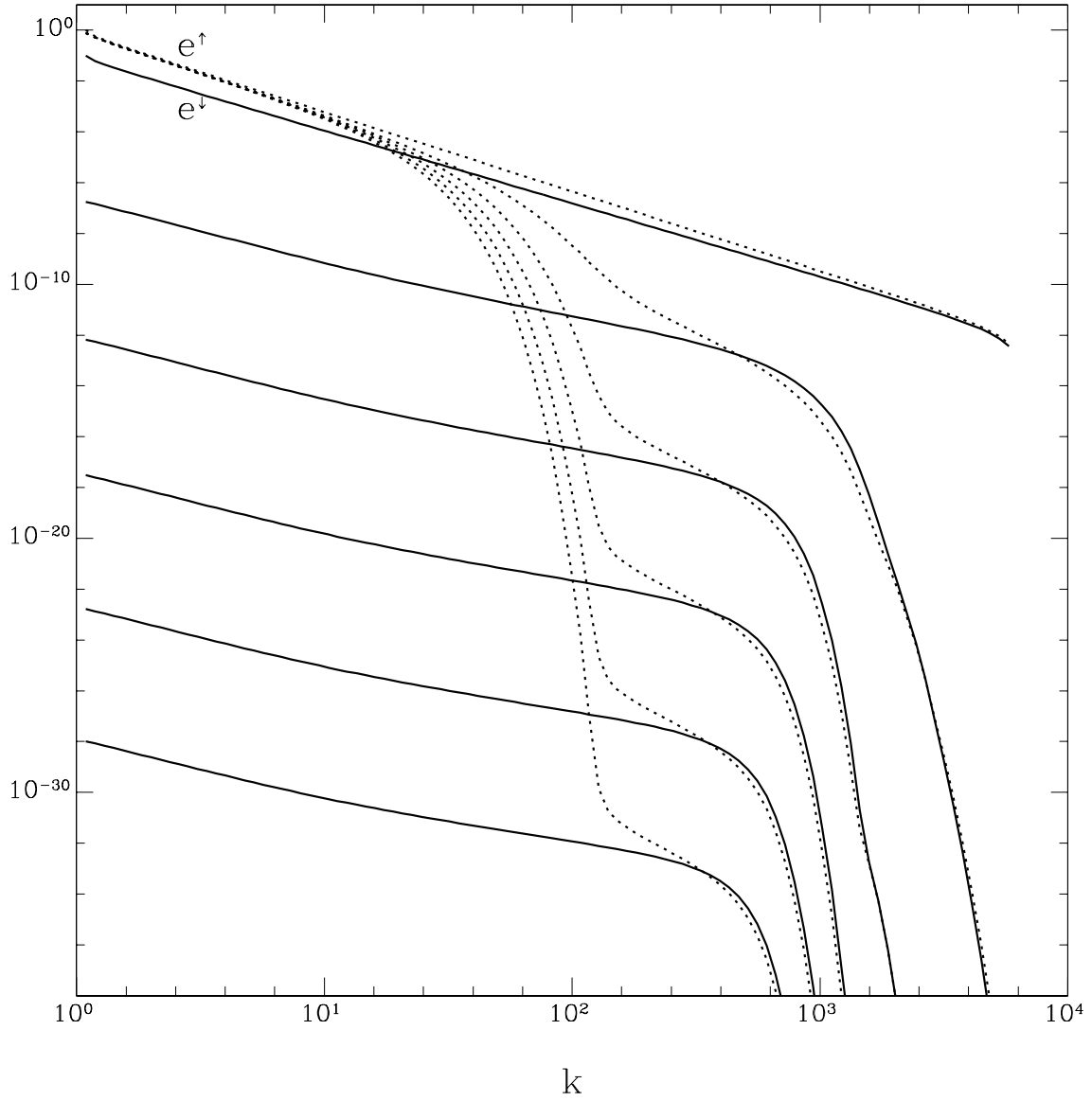


Fig. 4.— Decaying Simulation of Kinetic Equations

Spectra of e^\uparrow (dotted lines) and e^\downarrow (solid lines) at the following times: $t = 0, 25, 50, 75, 100, 125$ (from top to bottom).

where ke^\uparrow is the energy per unit k , and $\tilde{\epsilon}^\uparrow$ is the flux. This equation is similar in form to equation (50). Recall from §5.1 that we define the flux as the energy flow rate across a fixed $k \equiv |\mathbf{k}|$. It is the “1-D flux,” since we average over angles; similarly, ke^\uparrow is the “1-D energy density.” For $\tilde{\epsilon}^\uparrow$, we choose a form that depends on the following quantities evaluated at k : e^\downarrow , e^\uparrow , and $\partial_k e^\uparrow$. By contrast, the kinetic equations depend on e^\uparrow and e^\downarrow evaluated at a range of wavenumbers, so unlike the kinetic equations, the diffusion equations are exactly local in k . For the cascade time of the energy in the up waves to have the correct form (eq. [16]), i.e., $t_{\text{cas}}^\uparrow = (\lambda/w_\lambda^\downarrow)^2 (v_A/\Lambda) \sim (k^4 e^\downarrow)^{-1} (v_A/\Lambda)$, we choose

$$\tilde{\epsilon}^\uparrow = -\frac{\Lambda}{v_A} e^\downarrow k^{6-\beta} \frac{\partial}{\partial k} (k^{\beta+1} e^\uparrow), \quad (69)$$

where β remains to be specified. Of course the above relation for the flux gives the correct steady-state scaling: $e^\uparrow e^\downarrow \propto k^{-6}$. The evolution equations for e^\downarrow are the same as for e^\uparrow (eqs. [68] and [69]), with \uparrow 's and \downarrow 's interchanged.

With $e^\uparrow \propto k^{-(3+\alpha)}$, $e^\downarrow \propto k^{-(3-\alpha)}$, we can relate the steady-state fluxes to the energies:

$$\tilde{\epsilon}^\uparrow = \tilde{f}(\alpha) [k^6 e^\uparrow(k) e^\downarrow(k)] \frac{\Lambda}{v_A}, \quad (70)$$

$$\tilde{\epsilon}^\downarrow = \tilde{f}(-\alpha) [k^6 e^\uparrow(k) e^\downarrow(k)] \frac{\Lambda}{v_A}, \quad (71)$$

where

$$\tilde{f}(\alpha) = 2 + \alpha - \beta. \quad (72)$$

These relations are analogous to equations (29) and (30). To make the analogy closer, we choose β so that \tilde{f} has the same dependence on α as does f in the limit that the cascade is nearly balanced (i.e., $|\alpha| \ll 1$). Since $\tilde{\epsilon}^\uparrow/\tilde{\epsilon}^\downarrow = \tilde{f}(\alpha)/\tilde{f}(-\alpha) \simeq 1 + \alpha/(1 - \beta/2)$ in this limit, we see by comparison with equation (32) that we should choose $\beta = 0$.

Collecting results, our model equations are two coupled diffusion equations:

$$\frac{\partial}{\partial t} e^\uparrow = \frac{\Lambda}{v_A} \frac{1}{k} \frac{\partial}{\partial k} \left(e^\downarrow k^6 \frac{\partial}{\partial k} k e^\uparrow \right) - \nu k^2 e^\uparrow, \quad (73)$$

$$\frac{\partial}{\partial t} e^\downarrow = \frac{\Lambda}{v_A} \frac{1}{k} \frac{\partial}{\partial k} \left(e^\uparrow k^6 \frac{\partial}{\partial k} k e^\downarrow \right) - \nu k^2 e^\downarrow, \quad (74)$$

after including dissipative terms.

These equations, while much simpler than the kinetic equations, share many of the same features. Since the cascade time of the up-going waves is inversely proportional to the energy of the down-going waves (and vice versa), the argument for the pinning of the spectra in weak turbulence (see §3.3) applies here as well. Moreover, in steady state, these diffusion equations suffer from the same degeneracy as does the kinetic equation: the constancy of $\tilde{\epsilon}^\uparrow$ and $\tilde{\epsilon}^\downarrow$ is insufficient to determine the scaling of e^\uparrow or e^\downarrow separately. This degeneracy is partially broken by the dependence of the fluxes on the slopes (eqs. [70] and [71]); we have chosen this dependence so that it is the same as for the kinetic equations in the limit that the cascade is nearly balanced ($|\alpha| \ll 1$). In the following section, we present numerical simulations of these equations.

7.2. Numerical Simulations of Coupled Diffusion Equations

We run two simulations of the coupled diffusion equations. As with the kinetic simulations described in §6, the first simulation has fixed energy at the outer scale, and the second simulation has fixed flux. And, as before, $2\Lambda/v_A$ is set to unity, functions of k are evaluated at $k = 2^{i/8}$, $i = 1, \dots, 100$, and the viscosity is $\nu = 3 \cdot 10^{-5}$.

7.2.1. Fixed Energies at the Outer Scale

For our first simulation, we fix $e^\uparrow(k_{\text{out}}) = 0.63$ and $e^\downarrow(k_{\text{out}}) = 0.066$.¹⁵ The evolution is shown in Figure 5. It is very similar to the evolution of the kinetic simulation (Fig. 1). As before, the spectra are pinned quickly. And since, by design, the predicted steady state relations for the diffusion equations are the same as those for the kinetic equations (eqs. [61]–[66]), the steady state behaviour of the two simulations are nearly identical; compare Figures 5d and 1d. There are two differences worthy of note. First, the slopes of e^\uparrow and e^\downarrow do not have a spike near $k = k_{\text{out}}$. The presence of such a spike in the kinetic simulation is due to the extrapolation of the spectra to $k < k_{\text{out}}$ (see footnote 13). Since the diffusion equations are exactly local in k , such an extrapolation is unnecessary, and so the behaviour is much smoother near $k = k_{\text{out}}$. Second, in steady state, the diffusion simulations yield spectral slopes that change more gradually as a function of k near the dissipation scale; compare the top panel of Figure 1d with that of Figure 5d.

7.2.2. Fixed Fluxes

For the second simulation, we inject energy at $k = k_{\text{out}}$ at a fixed rate, equal to that found in steady state in the previous simulation. For the initial condition, we divide the previously found steady state value of e^\uparrow by 10, and we multiply e^\downarrow by 10. The evolution is shown in Figure 6. It is very similar to that found in the corresponding kinetic simulation (Figure 2).

8. Large Magnetic Prandtl Number

In incompressible MHD, diffusive dissipation of kinetic and magnetic energies is accounted for by addition of the terms $\nu \nabla^2 \mathbf{v}$ and $\eta \nabla^2 \mathbf{B}$ to the right-hand sides of equations (1) and (2), respectively, where ν is the viscosity and η is the resistivity. The magnetic Prandtl number is defined as

$$\text{Pr} \equiv \nu/\eta . \tag{75}$$

¹⁵We choose these numbers so that the spectra will have the same amplitude here as in the kinetic simulation; see footnote 14.

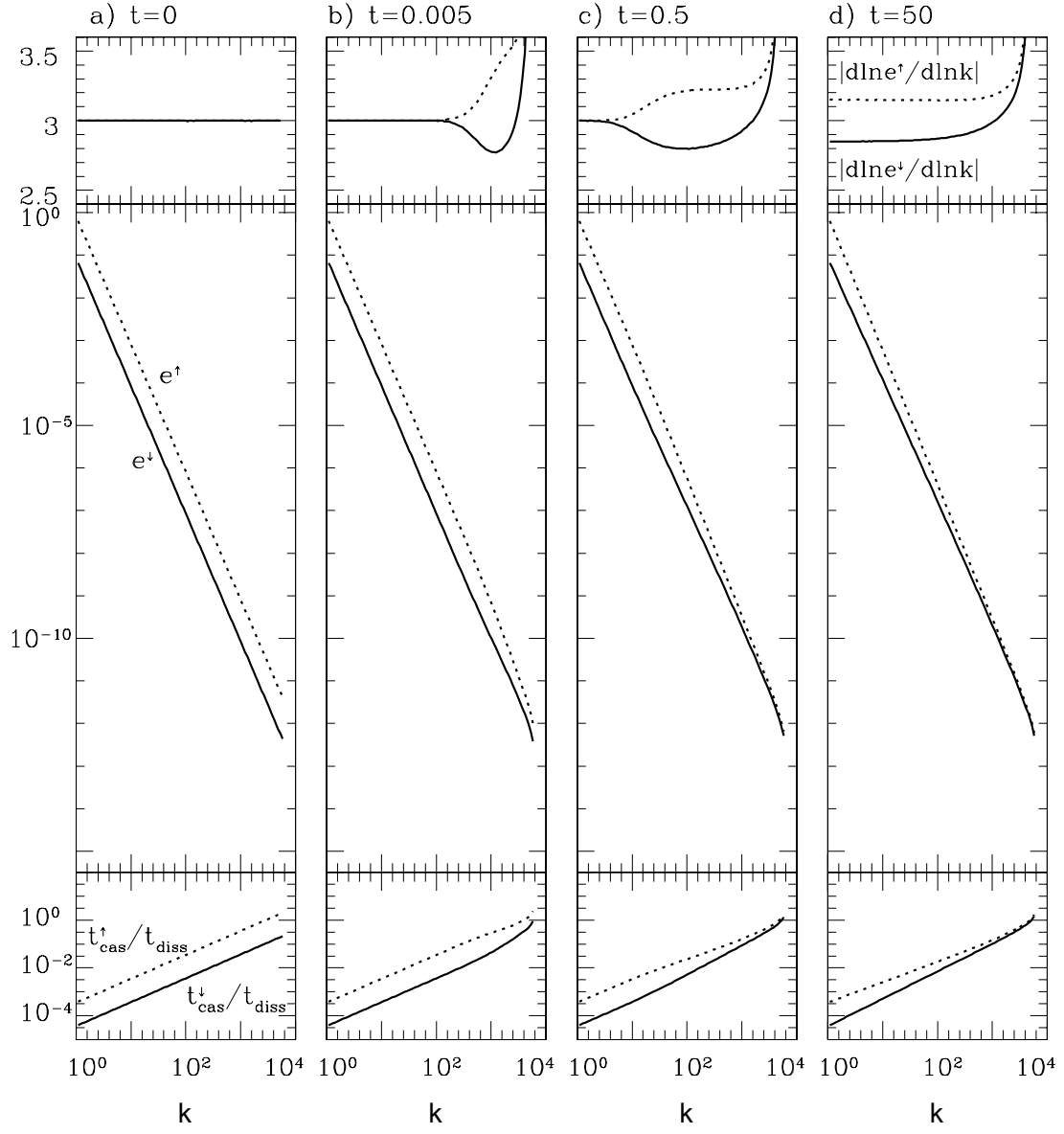


Fig. 5.— Simulation of Diffusion Equations with Fixed Energies at the Outer Scale

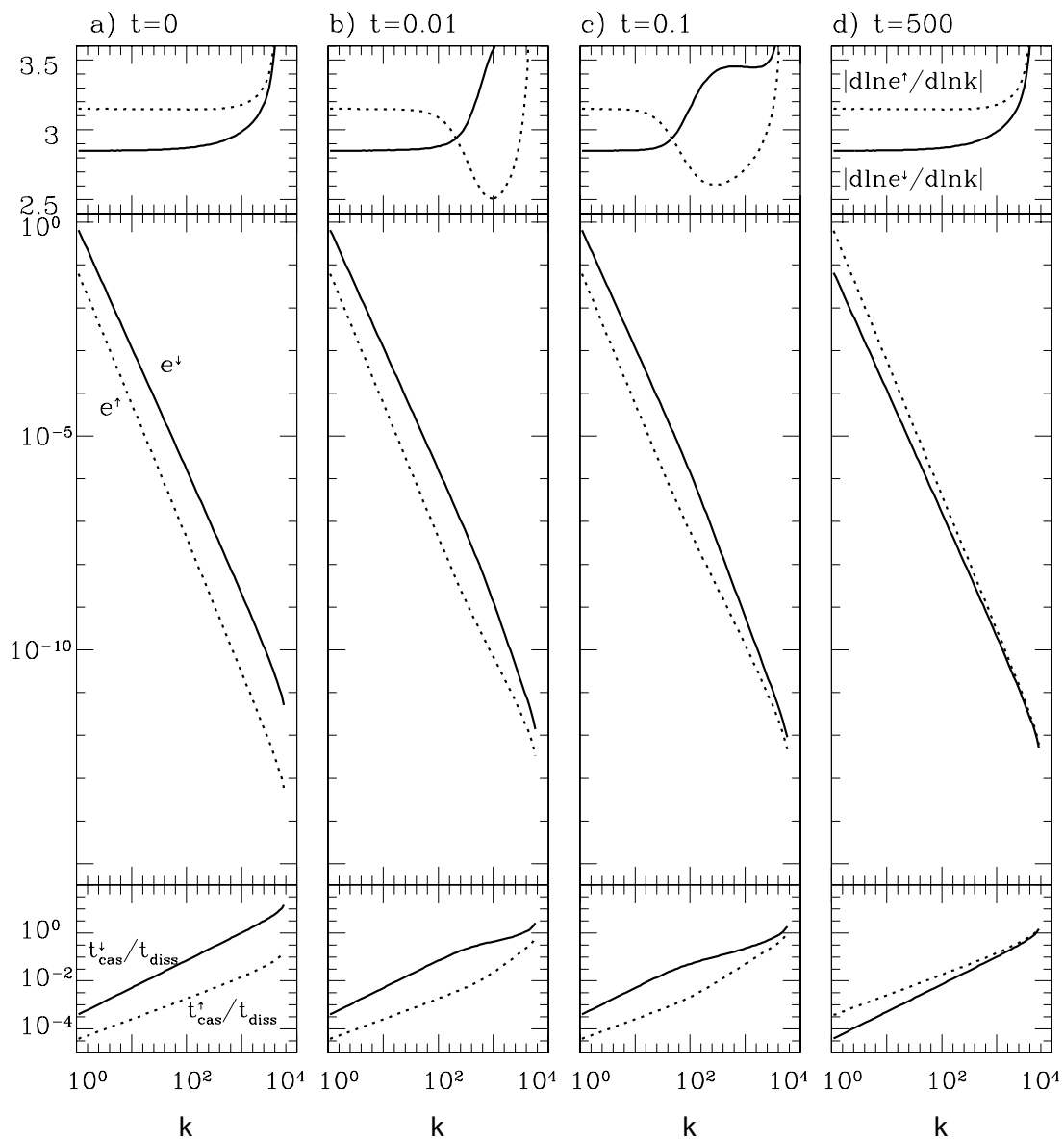


Fig. 6.— Simulation of Diffusion Equations with Fixed Fluxes

Until now, we have assumed that $\text{Pr}=1$. In this section, we examine weak MHD turbulence when $\text{Pr}\gg 1$.¹⁶

With arbitrary ν and η , the equation for \mathbf{w}^\uparrow (eq. [4]) becomes,

$$\partial_t \mathbf{w}^\uparrow + v_A \partial_z \mathbf{w}^\uparrow = -\mathbf{w}^\downarrow \cdot \nabla \mathbf{w}^\uparrow - \nabla P + \frac{1}{2}(\nu + \eta) \nabla^2 \mathbf{w}^\uparrow + \frac{1}{2}(\nu - \eta) \nabla^2 \mathbf{w}^\downarrow ; \quad (76)$$

the equation for \mathbf{w}^\downarrow is the same but with \uparrow and \downarrow interchanged, and $v_A \rightarrow -v_A$. To derive the kinetic equation for e^\uparrow , we first Fourier transform the above equation; the transformed dissipation terms are $-(k^2/2)(\nu + \eta)\mathbf{w}_k^\uparrow - (k^2/2)(\nu - \eta)\mathbf{w}_k^\downarrow$. When we take the dot product of the Fourier-transformed equation with \mathbf{w}_k^\uparrow , and then take the expectation value of the result, we can neglect the dissipation term proportional to $\langle \mathbf{w}_k^\uparrow \cdot \mathbf{w}_k^\downarrow \rangle$, since it is much smaller than the term proportional to $\langle (\mathbf{w}_k^\uparrow)^2 \rangle$. This is because in upgoing waves at fixed $z^\uparrow \equiv z - v_A t$ are uncorrelated with the downgoing ones (see §A.1). As a result, the kinetic equation for high magnetic Prandtl number is the same as that for $\text{Pr}=1$ (eq. [46]), but with $\nu k^2 e^\uparrow$ replaced by $(\nu + \eta)k^2 e^\uparrow/2 \simeq \nu k^2 e^\uparrow/2$. This might appear to be a surprising result. In the limit of vanishing η , the energy spectra are cut off below the viscous scale, i.e., the scale set by ν (eq. [27], within a factor of 2). One might have expected that the viscous scale should only affect the kinetic energy spectrum. Yet the magnetic energy spectrum is also cut off below the viscous scale. This can be understood as follows: upgoing waves each have equal magnetic and kinetic energies, and similarly for downgoing waves. As an up-wave with lengthscale slightly larger than the viscous scale is gradually cascaded to sub-viscous scales, its kinetic energy is dissipated by viscosity. Since the cascade time in weak turbulence is much longer than the waveperiod, as the up-wave’s kinetic energy is dissipated, its magnetic energy is converted into kinetic energy so that its magnetic and kinetic energies can remain nearly equal. As a result, both kinetic and magnetic energies are dissipated at the viscous scale.

9. Hyperviscosity and the Bottleneck Effect

In many different types of turbulent cascades, the energy spectrum exhibits a hump on scales slightly larger than the dissipation scale (e.g., Falkovich 1994). The hump is particularly pronounced in numerical simulations that use “hyperviscosity,” a trick whereby the diffusive term $\nu k^2 \mathbf{v}$ is replaced by $\nu_n k^n \mathbf{v}$, where n is typically 4 or 8, and ν_n is the hyperviscosity; the resistivity is modified in a similar manner (e.g., Borue & Orszag 1995, Biskamp 2000). With this trick, a smaller part of the spectrum is affected by dissipation, so a longer inertial range can be simulated with a fixed resolution. Although this trick does work, there is a problem: the spectrum on scales slightly larger than the dissipation scales is made flatter. The energy, in effect, is backed up. This is the bottleneck effect. It can be particularly problematic in simulations of strong MHD turbulence,

¹⁶Strong MHD turbulence with $\text{Pr}\gg 1$ occurs in many astrophysical settings.

where the energy backup can affect lengthscales considerably larger than the dissipative scales (Biskamp & Müller 2000).

This motivates us to investigate the bottleneck effect in weak turbulence. If the bottleneck effect appears, its interpretation will be simpler than in strong turbulence. We perform two simulations of the kinetic equation, one with hyperviscosity of the form $\nu_4 k^4$, and the other with $\nu_8 k^8$. In each simulation, we fix the energies at the outer scale, $e^\uparrow(k_{\text{out}}) = 1$, $e^\downarrow(k_{\text{out}}) = 0.1$, and allow the spectra to reach steady state. The steady state spectra of $k^6 e^\uparrow e^\downarrow$ are shown in Figure 7, offset for clarity. Also shown is the simulation with ordinary viscosity described in §6.1. From this figure it is apparent that weak turbulence suffers from the bottleneck effect; the effect becomes larger with increasing hyperviscous exponent.

The bottleneck effect can be understood as follows. Consider an up-wave with a lengthscale slightly larger than the dissipation scale. It is cascaded by down-waves that have slightly different lengthscales than its own. Hyperviscosity gives a sharper dissipative cutoff to the down-wave spectrum than ordinary viscosity. Therefore a hyperviscous simulation has fewer down-waves in the vicinity of the dissipation scale, and the cascade time of the up-wave is longer. For the up-wave energy flux to be independent of lengthscale, a longer cascade time implies a larger energy. As a result, the spectrum is flatter on scales slightly larger than dissipative ones. Falkovich (1994) offers a similar explanation for the bottleneck effect in hydro turbulence.

10. Discussion

In this paper we describe imbalanced weak turbulence and solve the steady state cascade. In a future paper, we will extend the result to the strong cascade. One of our ultimate goals is to develop a theory of imbalanced strong turbulence to apply to the solar wind, where imbalance is observed.

Although strong turbulence is more generally applicable than weak, the latter is a simple and illuminating model. There are a number of issues in strong turbulence that are not understood. Weak turbulence can be used as the first step in explaining them. For example, in this paper we examined the effect of a large magnetic Prandtl number on weak MHD turbulence. We also found that the bottleneck effect appears in weak turbulence, where its interpretation is straightforward. There are a number of other issues that we intend to investigate in weak turbulence as a prelude to understanding them in strong turbulence; for example, reconnection and the turbulent dynamo.

Research reported in this paper was supported by NSF grant AST-0098301.

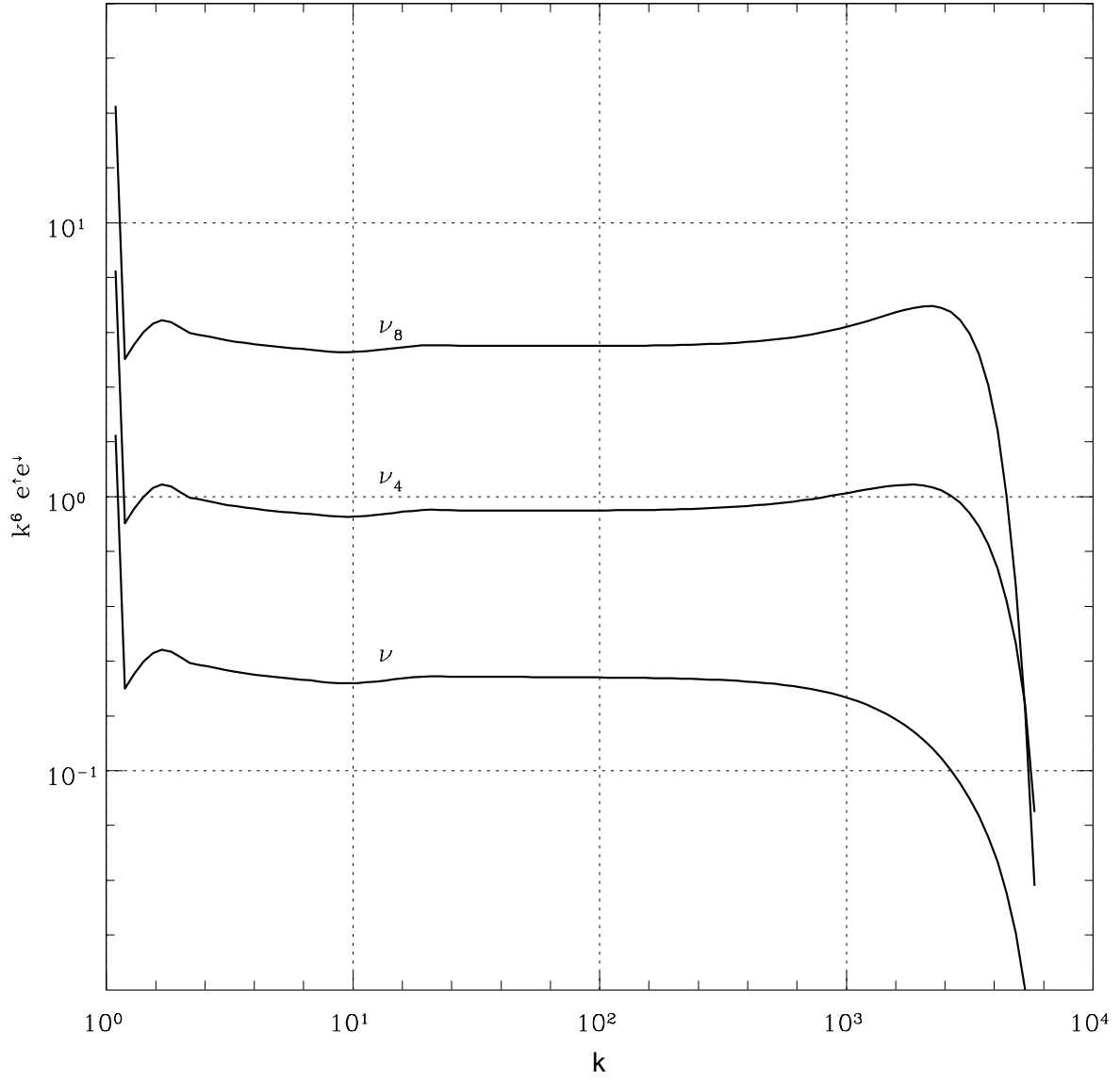


Fig. 7.— The Bottleneck Effect

Three spectra, offset for clarity; the top spectrum has viscous and resistive terms $\nu_8 k^8$, the middle has $\nu_4 k^4$, and the bottom has νk^2 .

A. Appendix: Kinetic Equation in Weak Turbulence

A.1. Preliminaries

Kinetic equations describing weak MHD turbulence are derived by Galtier et al. (2000, 2002). In this appendix, we present a more physical derivation. We compare the two derivations in §A.5.

We consider the evolution of \mathbf{w}^\uparrow in a plane that is transverse to $\hat{\mathbf{z}}$ and moving with velocity $v_A \hat{\mathbf{z}}$, i.e., with fixed $z^\uparrow \equiv z - v_A t$. Recall that $\hat{\mathbf{z}}$ is in the direction of the mean magnetic field. Changing variables from z to z^\uparrow in equation (8) gives

$$\left. \frac{\partial}{\partial t} \right|_{x,y,z^\uparrow} \mathbf{w}^\uparrow = -\mathbf{w}^\downarrow \cdot \nabla_\perp \mathbf{w}^\uparrow + \nabla_\perp \nabla_\perp^{-2} (\nabla_\perp \mathbf{w}^\downarrow : \nabla_\perp \mathbf{w}^\uparrow). \quad (\text{A1})$$

In weak turbulence, the parallel length over which disturbances are correlated, Λ , is small; in particular, in the time that an up-wave crosses a down-going wavepacket, $\Delta t \sim \Lambda/v_A$, its distortion is less than unity: $\Delta w_\lambda^\uparrow/w_\lambda^\uparrow \sim (w_\lambda^\downarrow/v_A)\Lambda/\lambda \ll 1$ (eq. [15]).¹⁷ Therefore, \mathbf{w}^\uparrow undergoes small uncorrelated changes each $\Delta t \sim \Lambda/v_A$, and its evolution is analogous to a random walk, with step-size $\Delta w_\lambda^\uparrow \sim w_\lambda^\uparrow (w_\lambda^\downarrow/v_A)\Lambda/\lambda \ll 1$. Our goal in this appendix is to quantify the random walk; the resulting equation is the kinetic equation. The kinetic equation is only valid when the turbulence is weak: its derivation hinges on the assumption that the time for up-waves to cascade is longer than the correlation time of down-waves at fixed z^\uparrow , i.e., that $(w_\lambda^\downarrow/v_A)\Lambda/\lambda \ll 1$.

Equation (A1) is linear in \mathbf{w}^\uparrow . Nonlinearity arises because \mathbf{w}^\uparrow modifies \mathbf{w}^\downarrow (through eq. [10]); this modification backreacts on \mathbf{w}^\uparrow through equation (A1). Nonetheless, this backreaction can be neglected when deriving the kinetic equation. The reason is as follows. Every $\Delta t \sim \Lambda/v_A$, the backreaction changes w_λ^\uparrow by $\sim w_\lambda^\uparrow [(w_\lambda^\downarrow/v_A)\Lambda/\lambda][(w_\lambda^\uparrow/v_A)\Lambda/\lambda]$, which is smaller than $\Delta w_\lambda^\uparrow$ by the small factor $(w_\lambda^\uparrow/v_A)\Lambda/\lambda \ll 1$. Furthermore, since this backreaction is uncorrelated on timescales larger than Λ/v_A , it only effects a small change in the step-size of the random walk.

Therefore, in deriving the kinetic equation, we interpret equation (A1) as a linear equation for \mathbf{w}^\uparrow (at fixed z^\uparrow); \mathbf{w}^\downarrow at fixed z^\uparrow is viewed as a function with known statistical properties. To simplify our derivation, we first solve a model problem: the linear random oscillator. The extension to weak turbulence will then be straightforward.

A.2. A Toy Problem: the Linear Random Oscillator

We consider the evolution of a simple random oscillator ψ :

$$\frac{d}{dt} \psi(t) = iA(t)\psi(t), \quad (\text{A2})$$

¹⁷We neglect the factor of 2 associated with the fact that the relative velocity of up and down waves is $2v_A$.

where ψ is a complex scalar and A is a real random variable; the factor i ensures that the energy $|\psi(t)|^2$ is conserved.¹⁸ Our goal is to calculate the evolution of $\langle\psi(t)\rangle$, where angled brackets denote an average over an ensemble of A 's, not over time. We assume that the values of A at two different times are statistically independent of each other whenever the two times are separated by more than the correlation time, τ_{corr} ; we make this more precise in footnote 20. For simplicity, we take A to have zero mean, $\langle A(t)\rangle = 0$; the extension to A with non-zero mean is trivial. We assume that the statistical properties of A —such as τ_{corr} and $A_{\text{rms}} \equiv \langle A^2 \rangle^{1/2}$ —vary only on timescales much larger than τ_{corr} . Note that ψ corresponds to w_λ^\uparrow in equation (A1); A corresponds to w_λ^\downarrow , or, more specifically, to $w_\lambda^\downarrow/\lambda$; and τ_{corr} corresponds to Λ/v_A .

There are two limiting regimes for the random oscillator, depending on whether $A_{\text{rms}}\tau_{\text{corr}}$ is less than or greater than unity. In the following, we take $A_{\text{rms}}\tau_{\text{corr}} \ll 1$; this regime corresponds to weak turbulence. The change in ψ within the time τ_{corr} is of order $A_{\text{rms}}\tau_{\text{corr}}\psi$, which is much smaller than ψ . Thus the correlation time of A is smaller than the “cascade time” of ψ . Since A is uncorrelated on timescales larger than τ_{corr} , ψ undergoes small uncorrelated changes each τ_{corr} , and thus its long-time evolution is a random walk. Intuitively, we expect that the time evolution of the statistical properties of ψ —in particular, $\langle\psi\rangle$ —can be represented by a differential equation. Our goal in this section is to derive the differential equation, and to understand the approximations that are made in deriving it.

The solution of equation (A2) is simply

$$\psi(t) = \psi(0) \cdot \exp(iA^t), \quad (\text{A3})$$

where $A^t \equiv \int_0^t A(t')dt'$. We expand as follows,

$$\psi(t) = \psi(0) \cdot (1 + iA^t - (AA^t)^t + \dots), \quad (\text{A4})$$

where $(AA^t)^t \equiv \int_0^t A(t') \int_0^{t'} A(t'')dt''dt'$; note that $(1/2)(A^t)^2 = (AA^t)^t$ is an identity for any $A(t)$. Equation (A4) may be thought of as an expansion in powers of A ; it is only valid for short times after $t = 0$.

We evaluate $\langle\psi(t)\rangle$ as follows. Since $A(t)$ is unaffected by $\psi(0)$, $A(t)$ and $\psi(0)$ are uncorrelated.¹⁹ So

$$\langle\psi(t)\rangle = \langle\psi(0)\rangle \cdot (1 + i\langle A^t \rangle - \langle (AA^t)^t \rangle + \dots). \quad (\text{A5})$$

Since $\langle A \rangle = 0$, we have $\langle A^t \rangle = 0$. Next, we consider $\langle (AA^t)^t \rangle$. The values of A at two different times “statistically overlap” only when the two times are separated by less than the correlation

¹⁸For a textbook discussion of the linear random oscillator, see van Kampen (1992).

¹⁹In fact, $A(t > 0)$ and $\psi(0)$ are slightly correlated: $\psi(0)$ is affected by $A(t_1 < 0)$, which is in turn correlated with $A(t_2 > 0)$ as long as $t_2 - t_1 \lesssim \tau_{\text{corr}}$. Nonetheless, in the limit $A_{\text{rms}}\tau_{\text{corr}} \ll 1$ that we are considering, ψ only changes by a small amount in the time τ_{corr} . So the correlation between $A(0 < t \lesssim \tau_{\text{corr}})$ and $\psi(0)$ is unimportant for the evolution of $\psi(t)$.

time; i.e., $\langle A(t')A(t' + \Delta t) \rangle$ is non-zero only if $\Delta t < \tau_{\text{corr}}$. Thus $\langle AA^t \rangle \simeq A_{\text{rms}}^2 \tau_{\text{corr}}$ when $t \gtrsim \tau_{\text{corr}}$, and

$$\langle (AA^t)^t \rangle \simeq A_{\text{rms}}^2 \tau_{\text{corr}} t .^{20} \quad (\text{A6})$$

Therefore

$$\langle \psi(t) \rangle \simeq \langle \psi(0) \rangle (1 - A_{\text{rms}}^2 \tau_{\text{corr}} t) , \quad \tau_{\text{corr}} \lesssim t \ll \tau_{\text{corr}} / (A_{\text{rms}} \tau_{\text{corr}})^2 . \quad (\text{A7})$$

Equivalently,

$$\frac{d}{dt} \langle \psi(t) \rangle = -A_{\text{rms}}^2 \tau_{\text{corr}} \langle \psi(t) \rangle , \quad \text{assuming } A_{\text{rms}} \tau_{\text{corr}} \ll 1 . \quad (\text{A8})$$

This equation is the main result of this section. Van Kampen (1992) gives a more mathematically rigorous derivation of it than we do. Equation (A8) can be understood as follows: since ψ changes by $\Delta\psi \sim A_{\text{rms}} \tau_{\text{corr}} \psi$ in the time τ_{corr} , then after N steps, each τ_{corr} long, the change in ψ is $\sqrt{N} \Delta\psi$. Thus for order unity changes in ψ , $(\psi/\Delta\psi)^2$ steps are required. The resulting time, the “cascade time,” is

$$\tau_{\text{cas}} = (\psi/\Delta\psi)^2 \tau_{\text{corr}} \sim 1 / (A_{\text{rms}}^2 \tau_{\text{corr}}) , \quad (\text{A9})$$

as in equation (A8), and $\tau_{\text{corr}}/\tau_{\text{cas}} \sim (A_{\text{rms}} \tau_{\text{corr}})^2 \ll 1$. Although $\langle \psi(t) \rangle$ decays to zero on the timescale τ_{cas} , the energy $|\psi|^2$ remains constant; the “cascade” of $\langle \psi \rangle$ is analogous to phase mixing.

We may now proceed to derive the kinetic equation in weak turbulence. Before doing so, we consider the linear random oscillator in more detail. If the reader is satisfied with the above derivation of equation (A8), the following subsection may be skipped.

A.2.1. *The Validity of Perturbation Theory and Goldreich & Sridhar (1997)*

Goldreich & Sridhar (1997) incorrectly claim that perturbation theory fails in weak turbulence, i.e., in their “intermediate” turbulence.²¹ We explain their claim and its resolution in the context of the linear random oscillator. In the process, we clarify the validity of the perturbation expansion.

We consider the terms neglected in equation (A7). For example, the fourth-order term is $\langle \psi^{(4)} \rangle / \langle \psi(0) \rangle = \langle \{A[A(AA^t)^t]^t\}^t \rangle$. In this quadruple time integral, A is evaluated at four different times. Whenever two of these times are separated by less than τ_{corr} , the values of A at these two times “statistically overlap,” and hence can give a non-zero contribution to the total integral. If two of the times are separated by less than τ_{corr} , and the other two times are also separated by

²⁰For this equation to be approximately valid, A must decorrelate sufficiently rapidly that $\langle A(t')A(t' + \Delta t) \rangle$ goes to zero faster than $1/\Delta t$ for large $\Delta t > \tau_{\text{corr}}$; otherwise, $\langle (AA^t)^t \rangle$ rises faster than the first power of t , and our derivation is invalid.

²¹A note on terminology: the turbulence that we and that Galtier et al. (2000) call “weak,” Goldreich & Sridhar (1997) call “intermediate.” They call it “intermediate” precisely because of their claim that perturbation theory is invalid.

less than τ_{corr} , then the integrand does not vanish, even if the first two times are separated from the second two times by more than τ_{corr} . So the quadruple time integral yields approximately $\langle \psi^{(4)} \rangle / \langle \psi(0) \rangle \sim (A_{\text{rms}}^2 \tau_{\text{corr}} t)^2 = (t/\tau_{\text{cas}})^2$.

Since $\langle \psi^{(2)} \rangle / \langle \psi(0) \rangle = -A_{\text{rms}}^2 \tau_{\text{corr}} t = -t/\tau_{\text{cas}}$, the contribution of the fourth-order term is as large as the second-order term after the time $t = \tau_{\text{cas}}$. Similarly, if we consider the contribution to $\langle \psi^{(2n)} \rangle / \langle \psi(0) \rangle$ from correlating pairs of A , the result is $\sim (t/\tau_{\text{cas}})^n$; so all terms are of comparable value when $t = \tau_{\text{cas}}$, and it seems that the lowest order term is inadequate. This, in effect, is the claim that Goldreich & Sridhar (1997) make in the context of weak turbulence.

It is incorrect; although equation (A7) for $\langle \psi(t) \rangle$ is only valid for $t \ll \tau_{\text{cas}}$, equation (A8) for $(d/dt) \langle \psi(t) \rangle$ is approximately valid for all times, with corrections of order powers of $\tau_{\text{corr}}/\tau_{\text{cas}} \ll 1$. Since $\psi(t)$ undergoes small uncorrelated changes every timestep of length τ_{corr} , we expect on physical grounds that the evolution of its statistical properties should be governed by a differential equation that is invariant under time translations.²² Equation (A8) is the only such equation whose small-time behaviour is given by equation (A7). Its right-hand side may be interpreted as the lowest term in a perturbative expansion in $\tau_{\text{corr}}/\tau_{\text{cas}}$. All of the contributions to $\langle \psi(t) \rangle$ that are of order $(t/\tau_{\text{cas}})^n$ must be derivable from equation (A8). For example, if $A_{\text{rms}}^2 \tau_{\text{corr}} \equiv 1/\tau_{\text{cas}}$ is constant, then equation (A8) has the solution $\langle \psi(t) \rangle / \langle \psi(0) \rangle = \exp(-t/\tau_{\text{cas}}) = 1 - t/\tau_{\text{cas}} + (1/2)(t/\tau_{\text{cas}})^2 + \dots$. Terms of order $(t/\tau_{\text{cas}})^n$ in $\langle \psi \rangle$ are generated from the lowest order term.

We can solve the one-dimensional oscillator exactly when $A(t)$ is Gaussian, and thereby illustrate the validity of equation (A8). If $A(t)$ is a zero-mean Gaussian random variable, then so is A^t , and $\langle \exp(iA^t) \rangle = \exp(-\langle (A^t)^2 \rangle / 2)$.²³ It follows from equation (A3) that

$$\langle \psi(t) \rangle = \langle \psi(0) \rangle \cdot \exp(-\langle (AA^t)^t \rangle), \quad (\text{A10})$$

assuming that $\langle \psi(0) \rangle$ and $A(t)$ are uncorrelated. Equivalently,

$$\frac{d}{dt} \langle \psi \rangle = -\langle AA^t \rangle \langle \psi \rangle, \quad (\text{A11})$$

which agrees with equation (A8) when $\langle AA^t \rangle = A_{\text{rms}}^2 \tau_{\text{corr}}$.

Although we are mainly concerned with the limit $A_{\text{rms}} \tau_{\text{corr}} \ll 1$, we conclude this subsection by briefly discussing the opposite limit, $A_{\text{rms}} \tau_{\text{corr}} \gg 1$. This limit sheds some light on strong turbulence, which corresponds to the case $A_{\text{rms}} \tau_{\text{corr}} \sim 1$. When $A_{\text{rms}} \tau_{\text{corr}} \gg 1$, perturbation theory is inapplicable because ψ does not undergo small uncorrelated changes every τ_{corr} . Rather, its cascade time is $\sim 1/A_{\text{rms}}$, which is much shorter than the correlation time of A . Therefore A is nearly constant in the time that $\langle \psi \rangle$ cascades. The inapplicability of perturbation theory makes

²²It should be invariant on the timescale τ_{corr} ; A_{rms} and τ_{corr} are effectively constants on this timescale.

²³Proof: a zero-mean Gaussian x has probability distribution $P(x) = (2\pi x_{\text{rms}}^2)^{-1/2} \exp(-x^2/2x_{\text{rms}}^2)$; so $\langle \exp(ix) \rangle = \int_{-\infty}^{\infty} P(x) \exp(ix) dx = \exp(-x_{\text{rms}}^2/2)$.

strong turbulence difficult, if not impossible, to solve. Nonetheless, we can solve the one-dimensional oscillator in the “strong” limit. Equations (A10) and (A11) are still valid, but $\langle AA^t \rangle \sim A_{\text{rms}}^2 t$, so $\langle \psi(t) \rangle \sim \langle \psi(0) \rangle \exp(-A_{\text{rms}}^2 t^2)$, and equation (A11) is not invariant under time translations. The time $t = 0$ is special because of our assumption that $\psi(0)$ and $A(t)$ are uncorrelated. This assumption, while innocuous for the “weak” oscillator, is crucial for the “strong” one.

A.3. Derivation of the Kinetic Equation

We derive the kinetic equation in Fourier space. We Fourier transform equation (A1) in x and y (but not z), denoting the transform of \mathbf{w}^\uparrow by $\mathbf{w}_{\mathbf{k}}^\uparrow$:

$$\mathbf{w}_{\mathbf{k}}^\uparrow \equiv \int d^2 \mathbf{x}_\perp \mathbf{w}^\uparrow \exp(-i\mathbf{k} \cdot \mathbf{x}_\perp), \quad (\text{A12})$$

where \mathbf{k} is purely transverse ($k_z \equiv 0$); similarly, $\mathbf{w}_{\mathbf{k}}^\downarrow$ is the Fourier transform of \mathbf{w}^\downarrow .

Since $\mathbf{w}_{\mathbf{k}}^\uparrow$ is perpendicular to both \mathbf{k} and $\hat{\mathbf{z}}$, it only represents a single degree of freedom. Hence it is convenient to define a scalar potential $\psi_{\mathbf{k}}^\uparrow$ by $\mathbf{w}_{\mathbf{k}}^\uparrow = i(\hat{\mathbf{k}} \times \hat{\mathbf{z}})\psi_{\mathbf{k}}^\uparrow$, with $\hat{\mathbf{k}} \equiv \mathbf{k}/k$. Similarly, $\mathbf{w}_{\mathbf{k}}^\downarrow = i(\hat{\mathbf{k}} \times \hat{\mathbf{z}})\psi_{\mathbf{k}}^\downarrow$. The Fourier transform of equation (A1) is then

$$\frac{\partial}{\partial t} \Big|_{\mathbf{k}, z^\uparrow} \psi_{\mathbf{k}}^\uparrow(t) = \int d^2 \mathbf{p} A_{\mathbf{k}, \mathbf{p}}(t) \psi_{\mathbf{p}}^\uparrow(t), \quad (\text{A13})$$

where

$$A_{\mathbf{k}, \mathbf{p}}(t) \equiv a_{\mathbf{k}, \mathbf{p}} \psi_{\mathbf{k}-\mathbf{p}}^\downarrow(t) \quad (\text{A14})$$

$$\equiv \frac{1}{(2\pi)^2} \hat{\mathbf{z}} \cdot (\mathbf{k} \times \mathbf{p}) \hat{\mathbf{k}} \cdot \hat{\mathbf{p}} \frac{\psi_{\mathbf{k}-\mathbf{p}}^\downarrow(t)}{|\mathbf{k}-\mathbf{p}|}. \quad (\text{A15})$$

We suppress the functional dependences of ψ^\uparrow and ψ^\downarrow on z^\uparrow because this equation is evaluated at fixed z^\uparrow ; in the following, we replace the partial time derivative by a total derivative, with the understanding that z^\uparrow is fixed.²⁴

We use angled brackets to denote an ensemble average, in a plane with fixed z^\uparrow . We define the spectral energy densities e^\uparrow and e^\downarrow as follows

$$\left\langle \mathbf{w}_{\mathbf{k}}^\uparrow(t) \cdot \mathbf{w}_{\mathbf{k}'}^\uparrow(t) \right\rangle = \left\langle \psi_{\mathbf{k}}^\uparrow(t) \psi_{\mathbf{k}'}^\uparrow(t) \right\rangle = e^\uparrow(\mathbf{k}, t) \delta(\mathbf{k} + \mathbf{k}') \quad (\text{A16})$$

$$\left\langle \mathbf{w}_{\mathbf{k}}^\downarrow(t) \cdot \mathbf{w}_{\mathbf{k}'}^\downarrow(t) \right\rangle = \left\langle \psi_{\mathbf{k}}^\downarrow(t) \psi_{\mathbf{k}'}^\downarrow(t) \right\rangle = e^\downarrow(\mathbf{k}, t) \delta(\mathbf{k} + \mathbf{k}'), \quad (\text{A17})$$

²⁴Since \mathbf{w}^\uparrow is real, $\mathbf{w}_{\mathbf{k}}^\uparrow = (\mathbf{w}_{-\mathbf{k}}^\uparrow)^*$, where $*$ denotes the complex conjugate, and so $\psi_{\mathbf{k}}^\uparrow = (\psi_{-\mathbf{k}}^\uparrow)^*$; similarly, $\psi_{\mathbf{k}}^\downarrow = (\psi_{-\mathbf{k}}^\downarrow)^*$. It follows that $A_{\mathbf{k}, \mathbf{p}} = A_{-\mathbf{k}, -\mathbf{p}}^*$ and $a_{\mathbf{k}, \mathbf{p}} = a_{-\mathbf{k}, -\mathbf{p}}^*$. The differential energy in up-waves within the k -space area $d^2 \mathbf{k}$ is proportional to $d^2 \mathbf{k} |\mathbf{w}_{\mathbf{k}}^\uparrow|^2 = d^2 \mathbf{k} |\psi_{\mathbf{k}}^\uparrow|^2$. Conservation of up-wave energy necessitates $A_{\mathbf{k}, \mathbf{p}} = -A_{\mathbf{p}, \mathbf{k}}^*$ and $a_{\mathbf{k}, \mathbf{p}} = -a_{\mathbf{p}, \mathbf{k}}^*$, as can be verified from equations (A14) and (A15).

where e^\uparrow and e^\downarrow are real; $\delta(\mathbf{k})$ is a two-dimensional Dirac delta-function that follows from homogeneity, i.e., from the assumption that $\langle \mathbf{w}^\uparrow(\mathbf{x}_\perp) \cdot \mathbf{w}^\uparrow(\mathbf{x}_\perp + \Delta\mathbf{x}_\perp) \rangle$ is independent of \mathbf{x}_\perp .

We shall derive the evolution equation for the bilinear quantity $\langle \psi_{\mathbf{k}}^\uparrow \psi_{\mathbf{k}'}^\uparrow \rangle$. From equation (A13),

$$\frac{d}{dt}[\psi_{\mathbf{k}}^\uparrow \psi_{\mathbf{k}'}^\uparrow] = \int d^2\mathbf{p} A_{\mathbf{k},\mathbf{p}} [\psi_{\mathbf{k}}^\uparrow \psi_{\mathbf{p}}^\uparrow] + (\mathbf{k} \leftrightarrow \mathbf{k}') , \quad (\text{A18})$$

where $(\mathbf{k} \leftrightarrow \mathbf{k}')$ represents a second term that is the same as the first, but with \mathbf{k} and \mathbf{k}' interchanged.

From §A.1, ψ^\downarrow (and hence $A_{\mathbf{k},\mathbf{p}}$) can be viewed as evolving independently of ψ^\uparrow , since the backreaction is negligible at fixed z^\uparrow . Therefore, equation (A18) is nearly identical to that of the simple random oscillator (eq. [A2]); $[\psi_{\mathbf{k}}^\uparrow \psi_{\mathbf{k}'}^\uparrow]$ and $A_{\mathbf{k},\mathbf{p}}$ in the above equation correspond to ψ and A , respectively, in equation (A2). Since ψ^\downarrow is a random function with zero mean and correlation time $\tau_{\text{corr}} = \Lambda/v_A$, so is $A_{\mathbf{k},\mathbf{p}}$. We solve equation (A18) in the same manner as we solved the random oscillator, using perturbation theory. Expanding in $A_{\mathbf{k},\mathbf{p}}$, we find to zeroth order:

$$[\psi_{\mathbf{k}}^\uparrow \psi_{\mathbf{k}'}^\uparrow]^{(0)} = \text{constant} . \quad (\text{A19})$$

To first order:

$$[\psi_{\mathbf{k}}^\uparrow \psi_{\mathbf{k}'}^\uparrow]^{(1)} = \int d^2\mathbf{p} A_{\mathbf{k},\mathbf{p}}^t [\psi_{\mathbf{k}}^\uparrow \psi_{\mathbf{p}}^\uparrow]^{(0)} + (\mathbf{k} \leftrightarrow \mathbf{k}') , \quad (\text{A20})$$

where $A_{\mathbf{k},\mathbf{p}}^t \equiv \int_0^t A_{\mathbf{k},\mathbf{p}}(t') dt'$. To second order:

$$[\psi_{\mathbf{k}}^\uparrow \psi_{\mathbf{k}'}^\uparrow]^{(2)} = \int d^2\mathbf{p} d^2\mathbf{q} \left\{ (A_{\mathbf{k},\mathbf{p}} A_{\mathbf{k}',\mathbf{q}}^t)^t [\psi_{\mathbf{p}}^\uparrow \psi_{\mathbf{q}}^\uparrow]^{(0)} + (A_{\mathbf{k},\mathbf{p}} A_{\mathbf{p},\mathbf{q}}^t)^t [\psi_{\mathbf{k}}^\uparrow \psi_{\mathbf{q}}^\uparrow]^{(0)} \right\} + (\mathbf{k} \leftrightarrow \mathbf{k}') . \quad (\text{A21})$$

The sum of these last three equations is directly analogous to equation (A4) for the simple oscillator. Using the same reasoning here as we did for the oscillator in deriving equation (A8), and assuming that the correlation time (Λ/v_A) is short, we take the time derivative of the expected value of equation (A21); we get, after setting $\langle AA^t \rangle = (\Lambda/v_A) \langle AA \rangle$ (with the appropriate subscripts on A), and after using equation (A16) and integrating out the delta functions on the right-hand side:

$$\delta(\mathbf{k} + \mathbf{k}') \frac{d}{dt} e^\uparrow(\mathbf{k}, t) = \frac{\Lambda}{v_A} \int d^2\mathbf{p} \left\{ \langle A_{\mathbf{k},\mathbf{p}} A_{\mathbf{k}',-\mathbf{p}} \rangle e^\uparrow(\mathbf{p}, t) + \langle A_{\mathbf{k},\mathbf{p}} A_{\mathbf{p},-\mathbf{k}'} \rangle e^\uparrow(\mathbf{k}', t) \right\} + (\mathbf{k} \leftrightarrow \mathbf{k}') . \quad (\text{A22})$$

We re-express this equation by using equations (A14) and (A17) and the relations $a_{\mathbf{k},\mathbf{p}} = a_{-\mathbf{k},-\mathbf{p}}^*$, $a_{\mathbf{k},\mathbf{p}} = -a_{\mathbf{p},\mathbf{k}}^*$ (from footnote 24), and $e^\uparrow(\mathbf{k}, t) = e^\uparrow(-\mathbf{k}, t)$:

$$\frac{d}{dt} e^\uparrow(\mathbf{k}, t) = 2 \frac{\Lambda}{v_A} \int d^2\mathbf{p} (e^\uparrow(\mathbf{p}, t) - e^\uparrow(\mathbf{k}, t)) |a_{\mathbf{k},\mathbf{p}}|^2 e^\downarrow(\mathbf{k} - \mathbf{p}, t) . \quad (\text{A23})$$

Since each upgoing plane with fixed z^\uparrow interacts with many statistically independent downgoing wavepackets before cascading, it is reasonable to assume isotropy in planes transverse to $\hat{\mathbf{z}}$; after

inserting equation (A15) for $a_{\mathbf{k},\mathbf{p}}$ and changing variables,

$$\frac{d}{dt}e^\uparrow(k, t) = \frac{\Lambda}{v_A}k^2 \int_0^\infty dk_2 k_2^3 \left[e^\uparrow(k_2, t) - e^\uparrow(k, t) \right] \int_0^{2\pi} d\theta \sin^2 \theta \cos^2 \theta \frac{e^\downarrow(k_1, t)}{k_1^2}, \quad (\text{A24})$$

where

$$k_1 \equiv (k^2 + k_2^2 - 2kk_2 \cos \theta)^{1/2}. \quad (\text{A25})$$

We have redefined Λ to absorb the factor of $4\pi^3$, i.e., $\Lambda/(4\pi^3) \rightarrow \Lambda$. Thus far, we have only considered a single plane with fixed z^\uparrow . If we assume that the turbulence is homogeneous in z , the z -average of the above equation is trivial since there is no explicit dependence on z . We can simply re-interpret angular brackets to denote z -averages in addition to an ensemble average.

We emphasize that our derivation of the kinetic equation (eq. [A24]) is only valid when the correlation time, Λ/v_A , is much smaller than the cascade time, $(v_A/\Lambda)(k^4 e^\uparrow)^{-1}$. Otherwise, equation (A22) does not follow from equation (A21).

A.4. Steady State Fluxes

In steady state, we set the right-hand side of equation (A24) to zero. We substitute power law solutions, $e^\uparrow(k) \propto k^{-(3+\alpha_\uparrow)}$, $e^\downarrow(k) \propto k^{-(3+\alpha_\downarrow)}$, in which case the right-hand side becomes

$$\left[e^\uparrow(k_0) e^\downarrow(k_0) k_0^{6+\alpha_\uparrow+\alpha_\downarrow} \frac{\Lambda}{v_A} \right] k^2 \int_0^k dk_2 k_2^3 \left(k_2^{-(3+\alpha_\uparrow)} - k^{-(3+\alpha_\uparrow)} \right) \left(1 - (k_2/k)^{\alpha_\uparrow+\alpha_\downarrow} \right) \cdot \int_0^{2\pi} d\theta \sin^2 \theta \cos^2 \theta \left(k^2 + k_2^2 - 2kk_2 \cos \theta \right)^{-(5+\alpha_\downarrow)/2}. \quad (\text{A26})$$

Note that the square-bracketed term is independent of k_0 . The above expression follows after breaking the k_2 integral into two pieces: one from 0 to k , and the second from k to ∞ . Then, the change of variables $k_2 \rightarrow k^2/k_2$ is made in the second piece (a ‘‘Zakharov transformation’’), so that its limits are now from 0 to k . Finally, this second piece is combined with the first.

In steady state, equation (A26) must vanish, so

$$\alpha_\downarrow = -\alpha_\uparrow. \quad (\text{A27})$$

Since $w_\lambda^\uparrow \sim (k^2 e^\uparrow)^{1/2} \propto k^{-(1+\alpha_\uparrow)/2}$, and similarly for w_λ^\downarrow , equation (A27) is equivalent to $w_\lambda^\uparrow w_\lambda^\downarrow \propto \lambda$ (eq. [19]). The vanishing of $\partial_t e^\downarrow$ in steady state yields the same relation as equation (A27), and so does not give new information.

The flux associated with e^\uparrow is given by integrating the right-hand side of equation (A24) over $d^2\mathbf{k}/(2\pi)$ from a particular k to infinity. The steady state flux is thus given by integrating equation (A26), with $\alpha_\downarrow = -\alpha_\uparrow$. The result of the flux integration is

$$\epsilon^\uparrow = f(\alpha_\uparrow) \left[e^\uparrow(k_0) e^\downarrow(k_0) k_0^6 \frac{\Lambda}{v_A} \right], \quad (\text{A28})$$

where $f(\alpha_\uparrow)$ is a dimensionless function of α_\uparrow :

$$f(\alpha_\uparrow) = \int_0^1 dx x^3 \ln x (x^{-(3+\alpha_\uparrow)} - 1) \int_0^{2\pi} d\theta \sin^2 \theta \cos^2 \theta (1 + x^2 - 2x \cos \theta)^{-(5-\alpha_\uparrow)/2}, \quad (\text{A29})$$

A technical note: although equation (A26) vanishes in steady state, its integral over $d^2\mathbf{k}$ gives a factor of $\alpha_\uparrow + \alpha_\downarrow$ in the denominator, which also vanishes in steady state. This 0/0 ambiguity can be resolved by considering the limit as $\alpha_\uparrow + \alpha_\downarrow \rightarrow 0$ (L’Hôpital’s rule).

Equation (A28) and the corresponding equation for ϵ^\downarrow , are equivalent to those in the heuristic discussion (eqs. [29] and [30]).

Galtier et al. (2000) plot the function $f(\alpha_\uparrow)$ after numerically integrating the steady-state flux integral.²⁵ They show that $-1 < \alpha_\uparrow < 1$, that the steeper spectrum always carries more flux (i.e., $f(\alpha_\uparrow)/f(-\alpha_\uparrow)$ is a monotonically increasing function of α_\uparrow), and that in the limit that $\alpha_\uparrow \rightarrow 1$, $\epsilon^\uparrow/\epsilon^\downarrow \rightarrow \infty$. (Clearly, this also implies that in the limit $\alpha_\uparrow \rightarrow -1$, $\epsilon^\uparrow/\epsilon^\downarrow \rightarrow 0$.) In §4.3.1, we explain the physical reason why $-1 < \alpha_\uparrow < 1$. When this condition is violated, the cascade becomes nonlocal. Galtier et al. (2000) find infinite fluxes when these inequalities are saturated because they consider an infinitely extended spectrum, which leads to unphysical results when the cascade is nonlocal.

As discussed in §4.2, in steady state we are primarily concerned with the case that the up- and down-going fluxes are comparable, so $|\alpha_\uparrow| \ll 1$. In this limit, we linearize f about $\alpha_\uparrow = 0$, yielding approximately

$$f(\alpha_\uparrow) \simeq f(0) \cdot (1 + 0.5\alpha_\uparrow) \quad , \quad |\alpha_\uparrow| \ll 1 \quad , \quad (\text{A30})$$

after numerical integrations of equation (A29). This result is used in §4.2 to calculate the energy spectra given the fluxes ϵ^\uparrow and ϵ^\downarrow . Although the value $f(0)$ is much less important than the dependence of f on α_\uparrow , we use it when discussing the results of our numerical simulations; it is given by

$$f(0) \simeq 1.87 \quad . \quad (\text{A31})$$

A.5. The Zero-Frequency Mode

Weak MHD turbulence is often described as being based on three-wave resonances, in which one of the three waves has zero frequency (e.g., Shebalin, Matthaeus, & Montgomery 1983, Galtier et al. 2000, 2002). However, the interpretation of a zero-frequency wave is unclear. After all, it should require an infinite amount of time for three interacting waves to “realize” that one of them has zero frequency. In this subsection, we clarify the role of the zero-frequency mode. In the process, we shall compare our derivation of the kinetic equation with that of Galtier et al. (2002).

²⁵More precisely, their figure 2 is proportional to $[f(\alpha_\uparrow)f(-\alpha_\uparrow)]^{-1/4}$, and their figure 3 shows $f(\alpha_\uparrow)/f(-\alpha_\uparrow)$.

Note that in our derivation in §A.3 we avoided discussing Fourier wavemodes, since we did not Fourier-transform in t or in z .

The evolution of the up-waves at fixed $z^\dagger \equiv z - v_A t$ is given in equation (A18). However, for clarity, in this subsection we shall consider the random oscillator instead (eq. [A2]):

$$d\psi/dt = iA\psi . \quad (\text{A32})$$

It is a simple matter to extend our discussion to weak MHD turbulence by replacing ψ with $\psi_{\mathbf{k}}^\dagger \psi_{\mathbf{k}'}$, replacing iA with $A_{\mathbf{k},\mathbf{p}}$, and summing over the appropriate indices.

In §A.2 we derived the equation for $\langle\psi\rangle$, assuming that the cascade time of $\langle\psi\rangle$ is longer than the correlation time of A :

$$d\langle\psi\rangle/dt = -\langle AA^t\rangle\langle\psi\rangle , \quad (\text{A33})$$

where $\langle AA^t\rangle \equiv \int_{t-T}^t \langle A(t)A(t')\rangle dt' \sim A_{\text{rms}}^2 \tau_{\text{corr}}$; the value of T is unimportant as long as $T > \tau_{\text{corr}}$.

We can see how the zero-frequency mode enters by re-writing $\langle AA^t\rangle$ in terms of \hat{A}_ω , the Fourier transform of A :

$$\langle AA^t\rangle = \int_{-\infty}^{\infty} \frac{d\omega'}{2\pi} \int_{-\infty}^{\infty} \frac{d\omega}{2\pi} \langle \hat{A}_{\omega'} \hat{A}_\omega \rangle e^{i\omega't} \int_{t-T}^t e^{i\omega t'} dt' . \quad (\text{A34})$$

To compare this result with that of Galtier et al. (2002), we shall use similar notation. We denote the power spectrum of \hat{A}_ω by q_ω :

$$\langle \hat{A}_{\omega'} \hat{A}_\omega \rangle \equiv q_\omega \delta(\omega' + \omega) ; \quad (\text{A35})$$

the Dirac-delta function results from the time-invariance of the statistical properties of A . We also define

$$\Delta(\omega) \equiv \frac{1}{i\omega} e^{i\omega t} (1 - e^{i\omega T}) . \quad (\text{A36})$$

With these two definitions, equation (A34) is

$$\langle AA^t\rangle = \int_{-\infty}^{\infty} \frac{d\omega}{4\pi^2} q_\omega \left[e^{-i\omega t} \Delta(\omega) \right] . \quad (\text{A37})$$

If this equation is inserted into equation (A33), the resulting equation is equivalent to equation (7) in Galtier et al. (2002). As these authors argue, when $T \rightarrow \infty$, $\exp(-i\omega t)\Delta(\omega) \rightarrow \pi\delta(\omega)$, so

$$\langle AA^t\rangle = \int_{-\infty}^{\infty} \frac{d\omega}{4\pi} q_\omega \delta(\omega) , \quad (\text{A38})$$

which corresponds to equation (8) in Galtier et al. (2002). From this expression, we can see why the zero-frequency mode enters: it is simply a consequence of the term $\langle AA^t\rangle$. It does not require an infinite time for $\langle\psi\rangle$ to interact with $q_{\omega=0}$; rather, the only quantity that enters into $q_{\omega=0}$ is the value of A within the time τ_{corr} of t . We can see this more clearly by explicitly writing the expression

for q_ω . Of course, the power spectrum q_ω is simply the Fourier-transform of the correlation function of A :

$$q_\omega = 4\pi \int_{-\infty}^0 e^{-i\omega\tau} \langle A(t)A(t+\tau) \rangle d\tau . \quad (\text{A39})$$

As long as $\omega \lesssim 1/\tau_{\text{corr}}$, we have $q_\omega \simeq 4\pi \langle AA^t \rangle$.

One of our reasons for discussing the Fourier-space picture in detail is that there have been a large number of confusing remarks about it in the literature. For example, Galtier et al. (2000, 2002) claim that, since the kinetic equation is apparently not applicable to the zero-frequency mode, there might be a “condensation” of zero-frequency modes. Since the zero-frequency mode is so important, this condensation might have dramatic implications for the cascade. However, as long as correlation times are shorter than cascade times, the kinetic equation gives a complete description of the turbulence, and is applicable to the zero-frequency mode as well, which is simply given by $q_{\omega=0} = 4\pi \langle AA^t \rangle$. For this not to be true, large-time correlations would have to build up in A (see eq. [A39]). Since A corresponds to ψ^\downarrow in weak MHD turbulence, large-time correlations at fixed z^\uparrow correspond to large-distance correlations along the z -direction. But it is impossible for two downgoing wavepackets, initially uncorrelated, to become correlated. This is because the equation for their evolution is linear: recall that in weak turbulence the backreaction term is negligible.

REFERENCES

- Biskamp, D. 1995, *Nonlinear Magnetohydrodynamics* (Cambridge: Cambridge University Press)
- Biskamp, D. 2000, *Magnetic Reconnection in Plasmas* (Cambridge: Cambridge University Press)
- Biskamp, D., & Müller, W.-C. 2000, *Phys. Plasmas*, 7, 4889
- Borue, V., & Orszag, S.A. 1995, *Europhys. Lett.*, 29(9), 687
- Cho, J., Lazarian, A., & Vishniac, E. 2002, *ApJ*, 564, 291
- Cho, J., & Vishniac, E. T. 2000, *ApJ*, 539, 273
- Dobrowolny, M., Mangeney, A., & Veltri, P. 1980, *Phys. Rev. Lett.*, 45, 144
- Falkovich, G. 1994, *Phys. Fluids*, 6, 1411
- Galtier, S., Nazarenko, S. V., Newell, A. C., & Pouquet, A. 2000, *J. Plasma Phys.*, 63, 447
- Galtier, S., Nazarenko, S. V., Newell, A. C., & Pouquet, A. 2002, *ApJ*, 564, L49
- Goldreich, P., & Sridhar, S. 1995, *ApJ*, 438, 763
- Goldreich, P., & Sridhar, S. 1997, *ApJ*, 485, 680

- Grappin, R., Pouquet, A., & Léorat, J. 1983, *A&A*, 126, 51
- Iroshnikov, P. 1963, *Soviet Astron.*, 7, 566
- Kraichnan, R. 1965, *Phys. Fluids*, 8, 1385
- Lithwick, Y., & Goldreich, P. 2001, *ApJ*, 562, 279
- Maron, J., & Goldreich, P. 2001, *ApJ*, 554, 1175
- Montgomery, D., & Matthaeus, W.H. 1995, *ApJ*, 447, 706
- Montgomery, D., & Turner, L. 1981, *Phys. Fluids*, 24, 825
- Ng, C.S., & Bhattacharjee, A. 1996, *ApJ*, 465, 845
- Ng, C.S., & Bhattacharjee, A. 1997, *Phys. Plasmas*, 4, 605
- Shebalin, J.V., Matthaeus, W.H., & Montgomery, D. 1983, *J. Plasma Phys.*, 29, 525
- Sridhar, S., & Goldreich, P. 1994, *ApJ*, 432, 612
- van Kampen, N.G. 1992, *Stochastic Processes in Physics and Chemistry*, Chapter XVI (Amsterdam: Elsevier Science Publishers)
- Zakharov, V.E., L'vov, V.S., & Falkovich, G. 1992, *Kolmogorov Spectra of Turbulence I* (Berlin: Springer)